
Article:
Wilkinson, S.W. orcid.org/0000-0002-4908-8766, Hannan Parker, A. orcid.org/0000-0002-8092-9930, Muench, A. orcid.org/0000-0002-9602-5944 et al. (12 more authors) (2023) Long-lasting memory of jasmonic acid-dependent immunity requires DNA demethylation and ARGONAUTE1. Nature Plants, 9 (1). pp. 81-95. ISSN 2055-026X

https://doi.org/10.1038/s41477-022-01313-9

Long-lasting memory of jasmonic acid-dependent immunity requires DNA demethylation and ARGONAUTE1

Wilkinson SW[1,*], Hannan Parker A[1], Muench A[1], Wilson RS[1], Hooshmand K[2], Henderson MA[1], Moffat EK[1], Rocha PSCF[1], Hipperson H[1], Stassen JHM[1], López Sánchez A[1], Fomsgaard IS[2], Krokene P[3], Mageroy MH[3] and Ton J[1,*]

[1] Plants, Photosynthesis and Soil, School of Biosciences, Institute for Sustainable Food, The University of Sheffield, Sheffield S10 2TN, United Kingdom

[2] Department of Agroecology, Aarhus University, DK-4200 Slagelse, Denmark

[3] Division for Biotechnology and Plant Health, Norwegian Institute of Bioeconomy Research (NIBIO), 1433 Ås, Norway

*Correspondence: j.ton@sheffield.ac.uk and samuel.wilkinson@sheffield.ac.uk

ABSTRACT

Stress can have long-lasting impacts on plants. Here, we report the long-term effects of the stress hormone jasmonic acid (JA) on the defence phenotype, transcriptome and DNA-methylome of Arabidopsis. Three weeks after transient JA signalling, 5-week-old plants retained induced resistance (IR) against herbivory but showed increased susceptibility to pathogens. Transcriptome analysis revealed long-term priming and/or up-regulation of JA-dependent defence genes but repression of ethylene- and salicylic acid-dependent genes. Long-term JA-IR was associated with shifts in glucosinolate composition and required MYC2/3/4 transcription factors, RNA-directed DNA methylation, the DNA demethylase ROS1, and the small RNA (sRNA)-binding protein AGO1. Although methylome analysis did not reveal consistent changes in DNA methylation near MYC2/3/4-controlled genes, JA-treated plants were specifically enriched with hypomethylated *ATREP2* transposable elements (TEs). Epigenomic characterisation of mutants and transgenic lines revealed that *ATREP2* TEs are regulated by RdDM and ROS1 and produce 21-nt sRNAs that bind to nuclear AGO1. Since *ATREP2* TEs are enriched with sequences from IR-related defence genes, our results suggest that AGO1-associated sRNAs from hypomethylated *ATREP2* TEs *trans*-regulate long-lasting memory of JA-dependent immunity.

INTRODUCTION

To resist pests and diseases, plants have evolved wide-ranging strategies which unfold over different timescales[1]. Pattern-triggered immunity (PTI) is an immediate immune response that protects against most attackers. However, specialised pests and diseases can suppress PTI, enabling them to initiate a parasitic interaction with their hosts[2–4]. The residual basal resistance is too weak to arrest specialised attackers but contributes to slowing down their colonisation[5]. Moreover, specific environmental signals can augment basal resistance. This so-called induced resistance (IR) is mediated by prolonged upregulation and/or priming of PTI-related defences[1], as PTI, basal resistance and IR share similar signalling pathways[3,5,6]. The defence hormones salicylic acid (SA) and jasmonic acid (JA) play central roles in these pathways[6,7]. While SA-dependent defences are mostly effective against (hemi-)biotrophic pathogens, JA activates defences against both necrotrophic pathogens and herbivores[3,7,8].

The immediate effects of JA signalling on defence gene expression are well documented. In *Arabidopsis thaliana* (Arabidopsis), bio-active JA-isoleucine (JA-Ile) stimulates binding of the F-box protein COI1 to JAZ repressor proteins[9–11]. This molecular interaction leads to ubiquitin-dependent degradation of JAZ proteins, which in turn results in induced activity of the defence regulatory transcription factors (TFs) MYC2/MYC3/MYC4 (MYC2/3/4) and EIN3/EIL3[9,11–14]. The MYC2/3/4 and EIN3/EIL1 branches of the JA response pathway are co-regulated by the plant hormones abscisic acid (ABA) and ethylene (ET), directing the JA pathway towards activation of defences against herbivory or necrotrophic pathogens, respectively[3,7,13,15–18].

Compared to the short-term effects of JA, little is known about the long-term impacts of JA, despite increasing evidence that transient exposure to stress can have long-lasting impacts on ecologically relevant life-history traits, such as growth rate, seed set and immune responsiveness[1]. It has even been reported that treatment of Arabidopsis and tomato with methyl jasmonate (MeJA) elicits transgenerational IR against chewing herbivores[19]. Although this response is not necessarily controlled by the same mechanisms as long-lasting IR within

58 the same generation, it demonstrates the ability of jasmonates to trigger an epigenetic IR
59 response. To date, the exact epigenetic mechanisms underpinning long-term JA-IR and their
60 associated impacts on global gene expression remain poorly understood.

61 In plants, cytosine (C) methylation, commonly referred to as DNA methylation, occurs at
62 three sequence contexts: CG, CHG and CHH (H being any base other than G) and
63 predominantly targets transposable elements (TEs) to silence their potentially damaging
64 effects on the genome[20]. The establishment of DNA methylation at TE-rich regions is under
65 antagonistic control by RNA-directed DNA methylation (RdDM)[21,22] and the DNA
66 demethylase ROS1[20,23]. There are different phases of RdDM. The initiation phase is
67 mechanistically connected to post-transcriptional gene silencing (PTGS) and involves the
68 generation of 21, 22 and 24-nt small interfering RNAs (siRNAs), which are derived from RNA
69 polymerase II (Pol II)-dependent transcripts and target initial DNA methylation to
70 unmethylated expressed loci[22,24]. Subsequently, RNA polymerase IV is recruited to establish
71 RdDM, during which predominantly 24-nt siRNAs guide the DNA methyltransferases
72 DRM1/2 to reinforce the DNA methylation[21,22]. Both the initiation and establishment phases
73 of RdDM require RNA polymerase V (Pol V) to generate scaffolding transcripts at the sites
74 being targeted for methylation[22,24]. Over recent years, evidence has emerged that RdDM and
75 ROS1 regulate plant defences against biotic stress[25–27].

76 Here, we have investigated the long-term consequences of JA seedling treatment on the
77 defence phenotype, transcriptome and DNA methylome of Arabidopsis. We show that the
78 long-term response to JA differs from the short-term response, involving IR against herbivory
79 but increased susceptibility to both necrotrophic and hemi-biotrophic pathogens. This long-
80 term JA-IR is associated with shifts in defence-related gene expression and glucosinolate
81 profiles, and is dependent on the MYC2/3/4 branch of the JA pathway, RdDM- and ROS1-
82 dependent DNA (de)methylation pathways, and the small RNA (sRNA)-binding effector
83 protein ARGONAUTE1 (AGO1). We furthermore show that long-term JA-IR is associated
84 with highly specific hypomethylation of TEs from the *ATREP2* family, which are controlled by

RdDM and ROS1, generate sRNAs that bind to nuclear AGO1, and are enriched with sequences that are homologous to defence genes displaying long-term priming/upregulation after JA treatment. We propose a model of plant immune memory that is driven by hypomethylated *ATREP2* TEs generating AGO1-associated sRNAs that augment MYC2/3/4-dependent defence against herbivores.

RESULTS

JA induces long-term resistance to a generalist herbivore and long-term susceptibility to both necrotrophic and hemi-biotrophic pathogens.

To examine the dynamics of the JA response over an extended time period, 2-week-old Arabidopsis seedlings were treated with water or 1 mM JA and analysed for JA-dependent *MYC2* and *VSP2* expression over a 3-week period (Fig. 1a,b). Both marker genes showed transient induction at 4 and 24 hours (hrs) post seedling treatment, after which their expression reverted to near baseline levels by 1 to 3 weeks (Fig. 1b). To assess the long-term effects of this transient JA signalling activity on the defence phenotype, we quantified resistance in 5-week-old plants, at 3 weeks after seedling treatment, against the generalist herbivore *Spodoptera littoralis* (*Sl*), the necrotrophic fungus *Plectosphaerella cucumerina* (*Pc*) and the hemi-biotrophic bacterial pathogen *Pseudomonas syringae* pv. *tomato* DC3000 (*Pst*; Fig. 1a). To compare these long-term effects with the short-term effects of JA, we also challenged an additional batch of 5-week-old plants with the same stresses at 1 day after treatment with water or 1 mM JA (Fig. 1a). As expected, the short-term effects of JA were characterised by IR against both *Sl* and *Pc*, as evidenced by a statistically significant reduction in larval weight and lesion diameter, respectively (Fig. 1c). Furthermore, JA treatment 1 day before *Pst* challenge increased bacterial leaf multiplication (Fig. 1c), supporting earlier reports that JA signalling suppresses SA-dependent resistance against (hemi-)biotrophic pathogens[28,29]. Interestingly, even though JA signalling activity had reverted to near basal levels at 1 week after JA seedling treatment (Fig. 1b), 5-week-old plants from JA-treated seedlings retained IR against *Sl* and induced susceptibility (IS) to *Pst* (Fig. 1d). Whereas, in contrast to the short-term JA response, plants from JA-treated seedlings displayed IS to the necrotrophic fungus *Pc* (Fig. 1d), indicating a fundamental difference between the short- and long-term effects of JA on Arabidopsis immunity. To verify the biological relevance of these contrasting long-term effects of JA on *Sl* and *Pc* resistance, we subjected seedlings to transient feeding by *Sl* larvae, which induces JA accumulation[30].

As observed after JA seedling treatment, seedling exposure to *Sl* feeding elicited long-term IR against *Sl* and long-term IS to *Pc* (Extended Data Fig. 1). Hence, the long-term effects of transient JA signalling activity at the seedling stage are biologically relevant and phenotypically different to the short-term JA response.

JA seedling treatment induces long-term priming of JA-dependent defences against herbivory but represses SA- and JA/ET-dependent defences against pathogens.

Since *MYC2* and *VSP2* expression reverted to near basal levels by 3 weeks after JA seedling treatment (Fig. 1b), we hypothesised that long-term JA-IR against *Sl* is based on priming of JA-dependent defence genes. To test this, we quantified expression of the MYC-dependent anti-insect acid phosphatase gene *VSP2* at 4, 8 and 24 hrs after challenging leaves from seedling-treated plants with water or 0.1 mM JA. Plants from JA-treated seedlings showed strongly augmented *VSP2* induction after JA challenge, confirming that JA seedling treatment causes long-term priming of antiherbivore defences (Fig. 1e). Conversely, plants from JA-treated seedlings showed reduced responsiveness of the SA-inducible antimicrobial *PR1* gene after challenge with 0.1 mM SA, as well as the JA/ET-dependent antifungal *PDF1.2* gene after challenge with a mixture of 0.1 mM JA + 0.1 mM of the ethylene precursor 1-aminocyclopropanecarboxylic acid (ACC; Fig. 1e). Hence, JA seedling treatment induces long-lasting priming of JA-inducible *VSP2* but long-term repression of SA-inducible *PR1* and JA/ET-inducible *PDF1.2*.

Long-term impacts of JA seedling treatment on the transcriptome.

To assess the long-term impacts of JA on the transcriptome, we performed mRNA sequencing (mRNA-seq) of leaves from 5-week-old plants of water- and JA-treated seedlings at 4 hrs after challenge with water or JA. This post-challenge timepoint was selected because (i) it showed the most pronounced impact of JA seedling treatment on marker gene expression (Fig. 1e) and (ii) previous high-resolution time-course analysis of global gene expression revealed that the most profound transcriptional changes in 5-week-

old plants occurred in the first few hours post treatment with MeJA[31]. Principal component analysis (PCA; Fig. 2a) and hierarchical cluster analysis (HCA; Fig. 2b) of normalised and transformed read counts revealed clear separation of samples by (pre)treatment (*n*=4; water seedling treatment and water challenge = W_W, JA seedling treatment and water challenge = JA_W, water seedling treatment and JA challenge = W_JA and JA seedling treatment and JA challenge = JA_JA). Hence, JA treatment of seedlings had a profoundly different impact on the transcriptome than JA challenge treatment of 5-week-old plants.

Since JA seedling treatment altered the resistance/susceptibility to JA-eliciting attackers (Fig. 1d), we hypothesised that JA seedling treatment modifies transcriptional responsiveness to secondary JA challenge. Accordingly, we selected genes showing a statistically significant interaction between JA seedling treatment and JA challenge (FDR-adjusted *p*-value < 0.01). The resulting 2,409 genes showed a range of different expression patterns (Supplementary Fig. 1 and Supplementary Data 1). To select for genes that are specifically associated with long-term JA-IR against *Sl*, we filtered the 2,409 genes for those that (i) were upregulated after JA challenge in plants from water-treated seedlings (W_JA > W_W) and (ii) showed augmented expression after JA challenge in plants from JA-treated seedlings compared to plants from water-treated seedlings (JA_JA > W_JA; Supplementary Data 2). HCA of the resulting 832 genes revealed four clusters, of which two (II and IV) displayed long-term upregulation and/or primed JA responsiveness in plants from JA-treated seedlings (Extended Data Fig. 2a and Fig. 2c). The 203 genes in clusters II and IV included the *VSP2* marker gene and were statistically enriched with gene ontology (GO) terms related to herbivore resistance, including “glucosinolate biosynthetic process” (Extended Data Fig. 2b, Fig. 2d and Supplementary Data 3, 4 and 5). To select genes associated with long-term JA-IS to *Pst*, we filtered the 2,409 genes for those which (i) were downregulated in response to JA challenge in plants from water-treated seedlings (W_JA < W_W) and (ii) showed reduced expression after JA challenge in plants from JA-treated seedlings compared to plants from water-treated seedlings (JA_JA < W_JA; Supplementary Data 6). HCA of the

resulting 904 genes revealed three clusters, of which two (V and VI) showed consistent short- and long-term repression by JA (Extended Data Fig. 2a and Fig. 2c). GO enrichment analysis of the 796 genes in clusters V and VI indicated enrichment of terms related to biotrophic pathogen resistance, including SA signalling (Extended Data Fig. 2b, Fig. 2d and Supplementary Data 7, 8 and 9). Finally, to select genes associated with long-term JA-IS to *Pc*, we filtered the 2,409 genes for those which (i) were upregulated after JA challenge in plants from water-treated seedlings (W_JA > W_W) and (ii) reduced in expression after JA challenge in plants from JA-treated seedlings compared to plants from water-treated seedlings (JA_JA < W_JA, Supplementary Data 10). HCA of the resulting 395 genes revealed one cluster (IX) with 144 genes showing long-term repression by JA and significant enrichment with numerous GO terms related to necrotrophic pathogen resistance (Extended Data Fig.2, Fig. 2c,d and Supplementary Data 11, 12 and 13). Thus, JA seedling treatment induces long-term priming/upregulation of genes related to JA-dependent defence against herbivores and long-term repression of SA- and ET-dependent genes against biotrophic and necrotrophic pathogens.

Long-term JA-IR against herbivory is dependent on MYC2/3/4 transcription factors.

To further investigate the transcriptional regulation of long-term JA-IR against *Sl*, we analysed the promoters (1 kb upstream from transcriptional start site; TSS) of the 203 IR-related genes for statistical enrichment with TF DNA binding motifs. Most strongly enriched motifs contained the canonical G-box motif (CACGTG; Fig. 3a and Supplementary Data 14), which functions as a core binding site for bHLH TFs, including JA regulatory TFs MYC2/3/4 (Fig. 3a and Supplementary Data 14)[17,32,33]. To validate involvement of MYC2/3/4 in long-term JA-IR against herbivory, we compared long- and short-term JA-IR against *Sl* in 5-week-old Col-0 and the *myc2 myc3 myc4* triple mutant (*mycT*)[17]. As reported previously[17,34], water-treated *mycT* plants allowed significantly higher larval growth than water-treated Col-0 plants (Fig. 3b), reflecting their compromised basal resistance against herbivory. Furthermore, JA-treated Col-0 plants allowed significantly lower rates of larval growth than water-treated Col-

0 plants, confirming their ability to express short- and long-term JA-IR against *Sl* (Fig. 3b). By contrast, JA treatment of *mycT* elicited neither short- nor long-term JA-IR against *Sl* (Fig. 3b), demonstrating a critical role of MYC2/3/4 TFs in both IR responses to this herbivore. Notably, *mycT* and Col-0 plants displayed similar growth reductions in plant growth after JA seedling treatment (Extended Data Fig. 3), indicating that long-term JA-IR is unrelated to JA-induced growth repression.

Long-term JA-IR against herbivory requires intact DNA (de)methylation pathways.

The defence-related phenotypes at 3 weeks after JA seedling treatment were expressed in leaves that were not present at the seedling stage, suggesting that there is a self-perpetuating resistance signal, which is transmitted through cell division into the newly formed leaves. Changes in DNA methylation offer a plausible mechanism, since these can be transmitted through cell division[35]. Furthermore, previous studies have indicated that changes in DNA methylation of TEs controls defence gene expression[26,36]. Since TE methylation in Arabidopsis is controlled by the antagonistic activities of RdDM and the DNA demethylase ROS1[20], we investigated whether this regulatory system is required for JA-IR by testing two previously characterised mutants in RdDM (*nrpe1-11*) and ROS1 (*ros1-4*)[26] for short- and long-term JA-IR against *Sl*. Both mutants expressed similar levels of basal resistance and short-term JA-IR as the wild-type (Col-0; Fig. 4a). By contrast, long-term JA-IR was strongly reduced in *nrpe1-11* and *ros1-4* compared to Col-0 and failed to cause a statistically significant reduction in larval development (Fig. 4a). All genotypes displayed similar reductions in plant growth after JA seedling treatment, indicating that the lack of JA-IR in *nrpe1-11* and *ros1-4* is unrelated to differences in JA-induced growth repression (Extended Data Fig. 3).

To obtain further evidence for the role of RdDM and ROS1 in long-term JA-IR against herbivory, we performed dual-choice assays to detect differences in attractiveness to *Sl* larvae between water- and JA-treated plants. At 20 hrs after release of the larvae in the choice arenas, a significantly higher number of *Sl* larvae preferred water-treated Col-0 plants

over JA-treated Col-0 plants, demonstrating that long-term JA-IR reduces the attractiveness to *Sl* (Fig. 4b). By contrast, *nrpe1-11* and *ros1-4* plants from water- and JA-treated seedlings attracted similar numbers of larvae (Fig. 4b), confirming that the *ros1-4* and *nrpe1-11* mutants are similarly affected in long-term JA-IR against herbivory. We therefore propose that long-term maintenance of JA-IR requires both RdDM and ROS1-dependent demethylation.

Long-term JA-IR is associated with ROS1-dependent changes in indole glucosinolates.

The 203 genes associated with long-term JA-IR against *Sl* were statistically enriched with genes controlling glucosinolate biosynthesis (Fig. 2 and Supplementary Data 5). Together with our finding that long-term JA-IR is controlled by DNA (de)methylation pathways (Fig. 4b), our results suggest that epigenetically controlled changes in the composition and size of the glucosinolate pool contribute to long-term JA-IR. To test this hypothesis, we used high performance liquid chromatography coupled with triple quadrupole mass spectrometry (HPLC-QqQ) to profile changes in glucosinolate content between WT and *ros1-4* plants following JA seedling treatment. JA had long-term effects on glucosinolate composition (Fig. 4d,e and Extended Data Fig. 4), predominantly altering concentrations of indole glucosinolates (IGs). The main IG compound, glucobrassicin (I3M), as well as its downstream derivative neoglucobrassicin (NMOI3M), showed a statistically significant increase in WT plants upon JA seedling treatment (Fig. 4d,e), while IG 4-methoxyglucobrassicin (4MOI3M) was statistically repressed by JA seedling treatment. Interestingly, the IG quantities and/or long-term changes in IG profiles were strongly attenuated (I3M and NMO13M) or absent (4MOI3M) in *ros1-4* (Fig. 4d,e and Extended Data Fig. 4). Hence, ROS1-dependent DNA hypomethylation is not only essential for long-term JA-IR (Fig. 4b,c) but also controls the associated shifts in IG composition (Fig. 4d,e).

The methylome of long-term JA-IR is characterised by variable DNA hypomethylation at TEs.

To assess the long-term impacts of JA on global DNA methylation, biologically replicated leaf samples (*n*=3) from 5-week-old plants at 3 weeks after seedling treatment were analysed by whole-genome bisulfite sequencing (WGBS). For all sequence contexts, the genome-wide weighted DNA methylation levels were comparable to previously reported values[37] (Extended Data Fig. 5a). Furthermore, although JA-treated samples showed on average marginally lower levels of genome-wide weighted DNA methylation, the differences were not statistically significant for any sequence context (Extended Data Fig. 5a). PCA and HCA of DNA methylation did not indicate consistent directional effects of JA seedling treatment. However both analyses revealed strongly increased variation in DNA methylation between replicate samples of JA-treated plants (Fig. 5a,b), which was driven by CHG and CHH sequence contexts (Fig. 5b and Extended Data Fig. 5b). Since non-CG methylation mostly occurs at intergenic TE sequences[38], we hypothesised that the increased variation in DNA methylation between plants from JA-treated seedlings occurs at TEs. To test this hypothesis, we selected differentially methylated regions (DMRs) between each individual JA replicate and all 3 water replicates (1JA_vs_3W). In contrast to statistical comparisons between 3 replicates from each treatment (3JA_vs_3W), which selects for DMRs that are consistently different across replicate JA samples, the 1JA_vs_3W comparisons allows for identification of statistically significant DMRs that are variable between replicate JA samples. For DNA methylation at all sequence contexts (all-C), the three 1JA_vs_3W comparisons identified 325, 291 and 260 DMRs, respectively (Fig. 5c and Supplementary Data 15 and 16). Although these DMRs were relatively small (average 41 bp), they were C-rich (average 13 C/DMR) and showed substantial shifts in methylation (average difference in methylation level of 43 percentage points; Supplementary Data 16). The 1JA_vs_3W comparisons for CHH context identified an average of 558 DMRs (Fig. 5c and Supplementary Data 15 and 16), while the comparisons for CHG and CG contexts yielded on average only 52 and 28

DMRs, respectively (Fig. 5c and Supplementary Data 15 and 16). These sequence-specific DMRs were relatively small (average 53, 50 and 42 bp for CHH, CHG and CG, respectively) but involved substantial changes in methylation levels (average difference of 45, 37 and 41 percentage points for CHH, CHG and CG, respectively; Supplementary Data 16). Notably, the majority of DMRs across all contexts and comparisons overlapped with TEs at intergenic regions and were hypomethylated in plants from JA-treated seedlings (Fig. 5c and Supplementary Data 16). Hence, the increased variation in DNA methylation by JA seedling treatment is largely driven by variable hypomethylation of TEs at non-CG context.

Long-term JA-IR is not associated with *cis*-acting DMRs within promoters of differentially expressed defence genes.

DNA methylation in gene promoters can influence binding of TFs to gene promoter motifs[20,39], which supports previous studies linking differential DNA methylation of promoters to changes in expression/responsiveness of the corresponding genes[25,26,40,41]. Although our global WGBS analysis suggests that JA-induced changes in DNA methylation occur at variable locations (Fig. 5a,b and Extended Data Fig. 5b), we examined whether DMRs from the different 1JA_vs_3W comparisons cluster within wider consensus regions of the same promoter regions. To this end, we searched for regions encompassing three DMRs, one from each of the 1JA_vs_3W comparisons (for details, see Supplementary Methods). At all-C context, we identified 2 consensus DMRs, which mapped to the same region on chromosome 1 and were not located at gene promoters (Supplementary Data 17). Increasing the maximum distance between individual DMRs from 100 to 500 bp did not yield additional consensus DMRs (Supplementary Data 17). Furthermore, we did not identify consensus DMRs at CG or CHG contexts and only identified 10 and 25 consensus DMRs at CHH context, using 100 and 500 bp maximum gaps, respectively (Supplementary Data 17). Although 7 and 19 of the latter CHH consensus DMRs were located within gene promoters, including *WRKY14* (AT1G30650), *GAT1* (AT1G08230) and *CAM7* (AT3G43810, Supplementary Data 17), none of these genes were differentially expressed in our

transcriptome analysis (Supplementary Data 1). We therefore conclude that the regulatory function of RdDM and ROS1 in long-term JA-IR against *Sl* (Fig. 4) does not primarily stem from *cis*-acting DMRs in promoters of primed and/or prolonged upregulated MYC2/3/4-dependent defence genes.

The *ATREP2* TE family is specifically targeted for long-term hypomethylation by JA seedling treatment.

Recent evidence suggests that DNA hypomethylation of TEs can stimulate defence gene expression via *trans*-regulatory mechanisms[1,36,42], which offers an alternative mechanism by which RdDM- and ROS1-dependent methylation controls long-term JA-IR. Various *trans*-acting mechanisms have been proposed, including activities by TE-derived small interfering RNAs (siRNAs)[1]. In the case of long-term JA-IR, however, such *trans*-regulating siRNAs would unlikely be generated by the same set of hypomethylated TEs as there were only a few consensus DMRs between plants from JA-treated seedlings (Supplementary Data 17). Since TEs within the same family and/or related families are highly homologous[43], we hypothesised that different TEs from the same taxonomic family can have similar *trans*-acting activities. To test this hypothesis, we first mined our data for TE (super)families that are significantly enriched with JA-induced DMRs. Strikingly, the *Helitron* TE family *ATREP2* stood out with on average a 11-fold (all-C) and 8-fold (CHH) enrichment with JA-induced DMRs compared to the genomic background of all TEs, which was highly significant for all 1JA_vs_3W comparisons at all-C and CHH contexts (Fig. 5d,e). These *ATREP2* DMRs were mostly hypomethylated and spread across all chromosomes (Extended Data Fig. 6), but none were part of consensus DMRs in the proximity of differentially expressed defence genes (Supplementary Data 1 and 17). Apart from *ATREP2*, there were a small number of additional TE families that were weakly enriched at JA-induced CHH DMRs (Fig. 5e and Extended Data Fig. 7a), but they did not show the same fold-enrichment and statistical significance as *ATREP2*, nor were they consistently enriched across all three 1JA_vs_3W all-C context comparisons (Fig. 5d,e and Extended Data Fig. 7a,b). For JA-induced DMRs at

CG and CHG contexts, there was weak enrichment of the *Gypsy* superfamily of LTR retrotransposons (Extended Data Fig. 7c,d). However, this enrichment was borderline statistically significant and did not translate to enrichment of specific TE families (Extended Data Fig. 7c,d). Thus, despite the variation in DNA hypomethylation, JA seedling treatment consistently targets TEs from the *ATREP2* family. Combined with the observed up-regulation and/or priming of MYC2/3/4-dependent defence genes (Figs. 2 and 3) and the critical role of RdDM- and ROS1-dependent DNA methylation in long-term JA-IR (Fig. 4), our WGBS results suggest that stochastic hypomethylation of members from the *ATREP2* TE family induce and/or prime JA-dependent defence genes via *trans*-acting mechanisms.

RdDM regulates DNA methylation at *ATREP2* TEs.

To further investigate the epigenetic control of long-term JA-IR, we focused on the regulation of *ATREP2* methylation by RdDM and ROS1. Tang and colleagues[23] previously categorised RdDM-targeted loci in Arabidopsis according to the degree by which they are antagonised by ROS1-dependent demethylation. Mining these data revealed that only 25 of all 164 *ATREP2* TEs overlapped with previously identified RdDM target loci (Extended Data Fig. 8a). Furthermore, the majority of the JA-induced DMRs from our methylome analysis did not correspond to RdDM targets (Fig. 5c and Extended Data Fig. 8b). These results were surprising considering the dependence of long-term JA-IR on RdDM/ROS1 (Fig. 4) and the strong impact of JA seedling treatment on DNA methylation at CHH sequence context (Fig. 5c). We therefore conducted our own WGBS analysis of shoot tissues from naïve Col-0, *nrpe1-11* and *ros1-4* plants (Extended Data Fig. 8c). Compared to members of two similarly sized class-2 TE families (*ATREP7* – 164 members and *TNAT1A* – 162 members) that were not targeted for DNA hypomethylation by JA seedling treatment (Fig. 5d,e), *ATREP2* TEs were highly methylated in Col-0 (Fig. 6a and Extended Data Fig. 8d-f). Moreover, *ATREP2* TEs exhibited dramatic reductions in DNA methylation by the *nrpe1-11* mutation (Fig. 6a and Extended Data Fig. 8d-f), whereas methylation levels remained high in the *ros1-4* mutant. These patterns extended across all JA-induced DMRs at both all-C and CHH contexts

(Extended Data Fig. 8g,h). Hence, *ATREP2*-enriched DMRs associated with long-term JA-IR show high levels of RdDM-dependent DNA methylation in naïve plants, which exposes them to ROS1-dependent DNA demethylation upon JA-induced stress.

ROS1 targets *ATREP2* TEs for demethylation.

We hypothesised that the lack of impact of the *ros1-4* mutation on *ATREP2* methylation (Fig. 6a) is because their DNA methylation level is already saturated in WT plants. To demonstrate that ROS1 can target *ATREP2* TEs for DNA demethylation, we transformed WT plants with a β-estradiol-inducible construct of YFP-tagged ROS1 (*XVE:ROS1-YFP*; Extended Data Fig. 9a), and used long-read Oxford Nanopore sequencing to assess impacts of ROS1 on *ATREP2* methylation. To ensure that *ROS1-YFP* was induced, plants were treated successively with 10 and 25 µM estradiol, respectively (Extended Data Fig. 9b). Compared to the dimethyl sulfoxide (DMSO) control, estradiol dramatically increased *ROS1* transcripts (Extended Data Fig. 9c), which was associated with ROS1-YFP accumulation in leaf cell nuclei and global hypomethylation at all sequence contexts (Extended Data Fig. 9d,e and Supplementary Data 18). Notably, estradiol induced widespread DNA hypomethylation in *ATREP2* TEs, which was statistically more pronounced compared to TEs from the two control families (*ATREP7* and *TNAT1A*; Fig. 6b and Extended Data Fig. 9f-h). Thus, ectopically induced ROS1 targets *ATREP2* TEs for DNA demethylation, which strengthens our notion that *ATREP2* methylation is antagonistically controlled by RdDM and ROS1.

AGO1 associates with sRNAs derived from *ATREP2* TEs and is essential for long-term JA-IR against herbivory.

Recently, Liu and colleagues reported that AGO1 associates with sRNAs in the nucleus and stimulates JA-dependent defence gene induction by changing the genes' chromatin structure and recruiting Pol II[44]. To examine whether AGO1-associated sRNAs from hypomethylated *ATREP2* TEs control long-term JA-IR, we mined their sRNA-sequencing data from nuclear

AGO1 of MeJA- and control-treated plants[44]. To enrich for AGO1-associated siRNAs, RNA sequences from other known RNA classes were removed from the analysis. As is shown in Extended Data Fig. 10a, *ATREP2*-derived sRNAs were strongly enriched at nuclear AGO1 compared to sRNAs from *ATREP7* and *TNAT1A,* which was particularly pronounced for 21-nt sRNAs. Moreover, *ATREP2*-derived sRNAs showed a statistically significant increase in the ratio of 21-nt sRNAs to 24-nt sRNAs (Extended Data Fig. 10b), suggesting that MeJA reduces Pol IV-dependent silencing and increases production of PTGS-dependent 21-nt sRNAs from Pol II-transcribed *ATREP2* TEs. Surprisingly, however, normalised counts of 21-nt and 24-nt sRNAs from all three TE families, including *ATREP2*, were lower in MeJA-treated plants compared to control-treated plants, which is difficult to reconcile with our hypothesis that JA increases the activity of resistance-inducing 21-nt sRNAs from *ATREP2*. However, it should be noted that the sRNA sequencing data from Liu and colleagues[44] are based on 10-day old agar-grown seedlings at 1 hour after MeJA treatment, making it difficult to draw direct comparisons to long-term IR in soil-grown plants at 3 weeks after JA seedling treatment.

To obtain further evidence for our hypothesis that *ATREP2*-derived sRNAs *trans*-regulate JA-dependent gene expression, we performed BLAST analysis[45] to assess sequence homology between *ATREP2* TEs and the 203 primed/up-regulated genes marking long-term JA-IR (Fig. 2c and Supplementary Data 4). Compared to *ATREP7* and *TNAT1A* TEs, the *ATREP2* TEs were enriched with sequences that are homologous to the 203 IR-related genes (Fig. 6c; Extended Data Figs. 10c,d). This enriched sequence complementarity was particularly pronounced for gene bodies of IR-related genes and was absent in 203 randomly selected control genes, as well as 203 stably expressed genes (Fig. 6c).

Finally, to confirm the function of AGO1 in long-term JA-IR, we quantified long-term JA-IR against *Sl* in two Arabidopsis lines carrying relatively weak mutant alleles of *AGO1* (*ago1-45* and *ago1-46*)[46], which were not majorly affected in growth and development. While the weight of *Sl* larvae reared on WT plants from JA-treated seedlings was significantly reduced

compared to larvae reared on naïve WT plants, this long-term JA-IR was absent in *ago1-45* and *ago1-46* plants (Fig. 6d). Hence, long-term JA-IR requires an intact AGO1 protein. Together, these results support a model wherein siRNAs from hypomethylated *ATREP2* TEs associate with nuclear AGO1 to prime and/or upregulate distant JA-dependent defence genes and mediate long-term JA-IR (Fig. 6e).

DISCUSSION

The immediate signalling response to JA has been studied extensively[47]. As a result, the pathways controlling short-term JA-IR against herbivores and necrotrophic pathogens, as well as the antagonistic effects of JA signalling on SA-dependent resistance against biotrophic pathogens, are well-documented[7,28,29]. By contrast, the long-term impacts of JA-dependent stress signalling have largely been overlooked, which does not do justice to the full breadth of plant adaptive strategies. Our study has shown that the long-term response to JA is phenotypically and mechanistically distinct from the short-term response (Fig. 1), involving changes in DNA methylation of specific TEs and the sRNA-binding protein AGO1 (Fig. 4-6).

IR is typically based on a combination of priming and prolonged upregulation of inducible defences[1]. In support of this, we identified 203 IR-related genes displaying long-term priming and/or prolonged upregulation after JA seedling treatment (Fig. 2c). Moreover, consistent with their role in IR against *Sl*, this cluster included genes with previously reported anti-herbivore activity (e.g.*VSP1* and *VSP2*)[48] and was statistically enriched with GO terms related to glucosinolate biosynthesis (Fig. 2d and Supplementary Data 4 and 5). Subsequent HPLC-QqQ profiling of glucosinolates confirmed that plants expressing long-term JA-IR show significant changes in IG composition (Fig. 4d,e and Extended Data Fig. 4). Previous studies have demonstrated that these anti-herbivore defences are controlled by MYC2/3/4 TFs[17,34]. Indeed, enrichment analysis of TF DNA-binding motifs in promoters of the 203 IR-related genes revealed strong enrichment with MYC-binding G-box motifs (Fig. 3a)[17,32], while the *mycT* mutant was impaired in long-term JA-IR against *Sl* (Fig. 3b). Hence, immune memory of long-term JA-IR is retained at the MYC2/3/4-dependent branch of the JA pathway, resulting in priming and/or prolonged up-regulation of anti-herbivore genes.

Recent evidence points to an important role of DNA methylation in plant immunity[25–27,36,42,49]. In most studies, however, epigenetic resistance is induced by artificial gene mutations affecting DNA methylation, which does not necessarily demonstrate biological relevance. By

contrast, our study shows that transient signalling activity by the plant's own stress hormone or caterpillar infestation induces long-term immune memory against herbivory, which is maintained in newly developed leaves and is dependent on DNA (de)methylation pathways (Fig. 4). Since DNA methylation of TEs is tightly controlled by RdDM and ROS1[20,23], our results indicate that long-term JA-IR requires RdDM- and ROS1-dependent changes in the methylation status of TEs. This conclusion is supported by our subsequent findings that long-term JA-IR is associated with genome-wide changes in non-CG methylation at TEs that are targeted by RdDM (Fig. 5c and Extended Data Fig. 8g,h).

Biotic stress typically leads to genome-wide DNA hypomethylation in plants[1,20,50]. For instance, both *Pst* infection and SA induce wide-spread hypomethylation in the genome of Arabidopsis[51,52], while MeJA treatment has been reported to induce DNA demethylation in *Brassica rapa*[53]. In most cases, stress-induced DNA hypomethylation is enriched at TE sequences[1,50,51,54,55], which supports our observation that the majority of JA-induced hypomethylation occurred at TEs in non-CG context (Fig. 5c). However, in contrast to previous studies, our WGBS analysis revealed considerable variability in TE hypomethylation by JA. Furthermore, the few consensus DMRs in our dataset were not located near MYC2/3/4-dependent defence genes that were primed/upregulated at 3 weeks after JA seedling treatment. Considering the critical role of RdDM and ROS1 in long-term JA-IR (Fig. 4), we propose that a variable pool of hypomethylated TEs stimulate the expression and/or responsiveness of MYC2/3/4-dependent defence genes via *trans*-acting mechanisms. Such mode of action is supported by independent reports that hypomethylated TEs can *trans*-regulate the expression and/or responsiveness of defence genes[1,26,36,42].

Different mechanisms have been proposed for *trans*-regulation of defence genes by hypomethylated TEs, including changes in long-range heterochromatic interactions and activities by TE-derived siRNAs[1,49]. Evidence for the latter mechanism comes from the recent discovery that siRNA-associated AGO1 stimulates JA-dependent defence gene expression through interaction with the SWI/SNF chromatin-remodelling complex and

recruitment of Pol II[44]. Our subsequent findings that long-term JA-IR is associated with hypomethylated DMRs at the *ATREP2* family of Helitron TEs (Fig. 5d,e) and that independent mutations in *AGO1* block long-term JA-IR against *Sl* (Fig. 6d) indicate that hypomethylated *ATREP2* TEs mediate this immune memory through a similar mechanism.

Involvement of Helitrons in stress responses has been reported in other eukaryotes. For example, Helitrons facilitate the heat shock responsiveness of nearby genes in *Caenorhabditis elegans*[56]. By contrast, the role of Helitrons in plant stress remains poorly documented, even though they are amongst the most abundant TEs in plants[57]. In this study, we have shown that *ATREP2* Helitron TEs are targeted for long-term DNA hypomethylation upon JA seedling treatment (Fig. 5d,e). Furthermore, they are highly methylated by RdDM in unstressed plants (Fig. 6a and Extended Data Fig. 8d-f) and become demethylated by ectopically induced ROS1 (Fig. 6b and Extended Data Fig. 9), indicating that *ATREP2* methylation is antagonistically controlled by RdDM and ROS1. We furthermore presented computational evidence that *ATREP2* TEs are enriched with sequences from IR-related defence genes (Fig. 6c) and generate 21-nt sRNAs with relatively high affinity to nuclear AGO1 (Extended Data Fig. 10a), which become enriched with 21-nt sRNAs after MeJA treatment (Extended Data Fig. 10b). This supports earlier findings that hypomethylated and reactivated Helitrons in stressed cell suspension cultures of Arabidopsis produce increased amounts of 21-nt sRNAs relative to 24-nt sRNAs[58]. Supported by our phenotypic evidence that mutations in RdDM, *ROS1* and *AGO1* block long-term JA-IR (Figs. 4b and 6d), our collective results suggest a model in which long-term JA-IR is controlled by ROS1-dependent demethylation of RdDM-targeted *ATREP2* TEs, which generate AGO1-binding 21-nt siRNAs that prime/upregulate distant defence genes (Fig. 6e). Since homologous members of the same TE family can generate similar siRNAs, this model also explains how variable patterns of DNA hypomethylation result in the same IR phenotype (Fig. 6e).

There are some results that do not fully align with our model of long-term JA-IR. For instance, it remains difficult to explain why *nrpe1-11* does not show increased basal resistance to *Sl* (Fig. 4b), despite its hypomethylated status of *ATREP2* TEs (Fig. 6a). We propose that the epigenetic impact of the *nrpe1-11* mutation differs from the more specific epigenetic impact of JA seedling treatment. Since DNA hypomethylation in *nrpe1-11* occurs across multiple TE families, this mutant will accumulate 21-nt sRNAs from a wider range of TEs than only *ATREP2* TEs, which could outcompete *ATREP2*-dervied sRNAs for AGO1 binding and prevent increased basal resistance to *Sl.* Alternatively, *ATREP2* TEs in *nrpe1-11* may be targeted by methylation-independent silencing mechanisms, which would prevent production of resistance-inducing sRNAs from hypomethylated *ATREP2* TEs. Another inconsistency stems from our analysis of previously published sequencing data of nuclear AGO1-associated sRNAs[44]. Our model proposes that jasmonate-induced *ATREP2* hypomethylation triggers the production of AGO1-associated 21/22-nt siRNAs. While the analysis of the data from Lui and Colleagues[44] confirmed a proportional increase in 21-nt sRNAs from *ATREP2* TEs after MeJA treatment (Extended Data Fig. 10b), the total count of AGO1-associated *ATREP2* sRNA reads was reduced by MeJA (Extended Data Fig. 10a). However, it should be noted that these data were obtained from agar-grown seedlings at 1 hour after MeJA treatment, whereas our experiments are based on soil-grown plants at 3 weeks after JA treatment. A more extensive analysis at multiple timepoints after JA treatment of soil-grown plants is required to identify the *ATREP2* derived and AGO1-associated sRNAs driving long-term JA-IR. Despite these discrepancies, our model is supported by independent studies demonstrating that TE hypomethylation stimulates the production of Pol-II-dependent TE transcripts[58,59], which are cleaved into 21/22-nt siRNAs by PTGS[22]. It is thus plausible that 21-nt siRNAs from hypomethylated *ATREP2* TEs accumulate and associate with nuclear AGO1 to mediate long-term JA-IR. Together with the complementary lines of evidence discussed above, we conclude that our study reveals a novel mode of epigenetic immune memory in plants (Fig. 6e). Future studies of the transient activities and interactions between MYC TFs, ROS1, RdDM proteins and the nuclear AGO1-

523 sRNA complex can provide further insights into the molecular and biochemical processes
524 underpinning this immune memory. Moreover, recent advances in epigenome editing
525 provide opportunities to exploit plant immune memory and generate crops that are better
526 prepared to resist future outbreaks by generalist herbivores.

METHODS

Biological material and growth conditions.

All Arabidopsis genotypes used in this study are in the genetic background of the accession Columbia (Col-0). Origin and confirmation of Arabidopsis genotypes are described in the Supplementary Methods. Arabidopsis seeds were stored at 4 °C in the dark and suspended in deionised H_2O (dH_2O) for 4 days to break dormancy, after which they were sown onto soil consisting of Levington Advance Pot & Bedding M3 compost (ICL) and sand in a 3:1 ratio (2:1 for experiments with *XVE:ROS1-YFP* plants) and, unless specified, cultivated under the following conditions: 8.5:15.5 hr day:night, 21 °C, 45-70% relative humidity (RH) and 100-250 µE m^{-2} s^{-1}.

Plectosphaerella cucumerina strain *BMM* (*Pc*) was kindly provided by Professor Brigitte Mauch-Mani (University of Neuchâtel, Switzerland) and *Pseudomonas syringae* pv. *tomato* DC3000 *luxCDABE* (*Pst*) was kindly provided by Dr Jun Fan (John Innes Centre, UK)[60]. *Spodoptera littoralis* (*Sl*) eggs were kindly provided by Professor Ted Turlings (University of Neuchâtel, Switzerland). Details about the cultivation of pathogens and insect rearing are presented in the Supplementary Methods.

Plant treatments.

Chemical origin and preparation of chemical treatments are detailed in the Supplementary Methods. Pre-treatments with JA were performed with either 2-week-old seedlings (long-term experiments; 3 weeks prior to challenge) or nearly 5-week-old plants (short-term experiments; 1 day prior to challenge). The long-term impact of JA pre-treatment on plant growth was analysed in 5-week-old plants using non-destructive hyperspectral quantification of rosette surface area, as detailed in the Supplementary Methods. Challenge treatments were performed when plants were 5 weeks old. *XVE:ROS1-YFP* plants were sprayed with 10 µM estradiol 14 days after sowing and 25 µM estradiol 18 days after sowing. As a control, *XVE:ROS1-YFP* plants were sprayed with dH_2O supplemented using the same percentage

(v/v) dimethyl sulfoxide (DMSO) as the estradiol treatments. All chemical treatments were performed by spraying plants until the leaf surfaces were entirely covered by liquid. To test the long-term effects of herbivory, 2nd instar *Sl* larvae were placed on 2-week-old Col-0 plants and allowed to feed until 50-75% of above ground tissue had been removed. To prevent (lethal) damage to the hypocotyl and encourage larvae to feed from cotyledons and leaves, soil was piled around the hypocotyl and a 15 ml falcon tube was placed over each plant. These protective measures were also applied to control plants without larvae.

Quantification of JA-IR against pathogens and herbivores.

To quantify IR against *Pc*, 4 leaves of a comparable physiological age from 5-week-old plants (17-22 plants per treatment-genotype combination) were droplet-inoculated with 6 µl droplets of inoculum (5×10^6 spores/ml H_2O), as described previously[61,62]. Inoculated plants were maintained at 100% RH until lesion diameters were measured at 6-8 days post inoculation (dpi) and averaged into a single value per plant (unit of biological replication).

To quantify IR against *Pst*, 4 leaves of a comparable physiological age from 5-week-old plants (9-12 plants per treatment-genotype combination) were syringe-infiltrated with a 10 mM $MgSO_4$ suspension of *Pst* bacteria at OD_{600nm} = 0.0002[63]. Plants were maintained at 80-100% RH. At 3 dpi, 4 leaf disks (0.2 cm^2) were harvested per plant and pooled (unit of biological replication). Leaf discs were homogenised in 10 mM $MgSO_4$ and 5-fold dilution series were plated on KB agar plates supplemented with rifampicin (50 µg ml^{-1}) and kanamycin (50 µg ml^{-1}). Plates were incubated at 28 °C for 20 hrs and 4 °C for 17 hrs prior to colony counting. Colonisation was expressed as the number of colony forming units (cfu's) per cm^2 of leaf tissue.

To quantify growth of *Sl* larvae in no-choice IR assays, 5-week-old plants (15-24 plants per treatment-genotype combination) were grown individually in 425 ml transparent plastic cups with three 0.8 cm^2 holes drilled in the bottom to allow for water drainage. A single *Sl* neonate larva was placed onto each plant with a fine paintbrush and a transparent lid was placed on

each cup. Larvae were removed and weighed when complete consumption of the most susceptible treatment group was imminent or after 7 days, whichever came first. The weight of a single larva fed on an individual plant represented the unit of biological replication.

To quantify *Sl* attractiveness in dual-choice assays, 5-week-old plants were placed in the dual-choice arenas (18 per genotype) at 3 weeks after seedling treatment. Every arena consisted of two plants from water- or JA-treated seedlings of the same genotype in separate pots, which were positioned within a 1 L transparent plastic container that was backfilled with soil and separated by a 30 mm inverted Petri dish lid (the 'arena'). Five 2nd-3rd instar *Sl* larvae were placed into the arena, after which containers were closed with pin-pricked lids. After 20 hrs, the position of each larva was recorded. If larvae were not on a plant or the soil immediately under it, they were recorded as no choice.

Construction and microscopy analysis of *XVE:ROS1-YFP* plants.

The *XVE:ROS1-YFP* binary plasmid was constructed using a MultiSite Gateway recombination reaction with the pENTR/D-TOPO plasmid containing the *ROS1* genomic sequence, the *XVE*-containing entry plasmid p1R4-p35S:XVE[64,65], the *VenusYFP*-containing entry plasmid p2R3a-VenusYFP-3AT (Addgene, #71269)[64] and the binary destination plasmid pCAM-kan0R4R3 (Addgene, #71275)[64], following manufacturer's recommendations (MultiSite Gateway Three-Fragment Vector Construction Kit; Thermo Fisher Scientific, 12537-023). Bacterial and plant transformations are detailed in the Supplementary Methods. To verify functionality of the *XVE:ROS1-YFP* plasmid, 19-day-old transgenic plants were analysed for YFP fluorescence at 24 hrs after treatment with 25 μM estradiol or 0.05% DMSO (control), and 5 days after treatment with 10 μM estradiol or 0.02% DMSO (control), as outlined in Extended Data Fig. 9b. Additional details about the fluorescence microscopy are presented in the Supplementary Methods.

Glucosinolate profiling.

Leaf material for glucosinolate profiling was collected from 5-week-old WT and *ros1-4* plants pre-treated with water (control) or JA (1 mM) as 2-week-old seedlings. Biologically replicated samples (*n*=8) consisted of 8 leaves of similar age, collected from 2 plants (4 leaves/plant). Leaf tissue was flash frozen and then lyophilized. Extraction and quantification of glucosinolates was performed as described previously[66] and as detailed in the Supplementary Methods.

Gene expression analysis.

Details about the timing and replication of collected leaf samples, RNA extraction, reverse transcription, and quantitative PCR are described in the Supplementary Methods. Library preparation and sequencing was performed by BGI Genomics, as detailed in the Supplementary Methods. Sequencing was performed with the BGISEQ-500 platform functioning in its single end mode. Across all 16 samples, 598 million 50 bp single-end clean reads were generated, with an average of 37.4 million clean reads per sample (Supplementary Data 19). Details about read alignment, read counting, statistical analysis of differentially expressed genes, enrichment analysis of gene ontology (GO) terms, and transcription factor DNA-binding motif enrichment analysis, are presented in the Supplementary Methods.

DNA methylation analysis.

Whole-genome bisulphite sequencing (WGBS) analysis was performed on samples from two separate experiments. The experiment to determine global DNA methylation patterns associated with long-term JA-IR was based on leaf material collected from 5-week-old plants, which had been treated with water (control) or 1 mM JA as 2-week-old seedlings. Biologically replicated samples (*n*=3) consisted of 12 leaves of similar age collected from 6 plants (2 leaves/plant) of a single tray. The experiment to determine impacts of the *nrpe1-11* and *ros1-4* mutations on global DNA methylation was based on 2/3-week-old Col-0, *nrpe1-*

11 and *ros1-4* plants grown at 16:8 hr day:night, 22 °C, 60% relative humidity (RH) and 150 µE m^{-2} s^{-1}. Biologically replicated samples for each genotype (*n*=4) consisted of 28-35 plants of a similar age. Genomic DNA was extracted using the GenElute Plant Genomic DNA Miniprep Kit (Sigma-Aldrich). Library preparation and sequencing was performed by BGI Genomics using their standard WGBS protocol. The sequencing of 150 bp paired-end reads was performed with a HiSeq X Ten System (Illumina). Statistics for the WGBS data are provided in Supplementary Data 20 and 21. Details about read alignment, methylation calling, estimation of genome-wide methylation levels, analysis of global DNA methylation patterns, analysis of differentially methylation regions (DMRs), calculation of DNA methylation levels at DMRs and TEs, and analysis of type-I/type-II RdDM targets[23] in DMRs and TEs, are described in the Supplementary Methods. Methylome analysis by long-read Oxford Nanopore sequencing to assess impacts of ectopically induced ROS1:YFP on DNA methylation was performed 48 hrs after the second spray-treatment with DMSO/estradiol (Extended Data Fig. 9b). Library preparation, sequencing with an Oxford Nanopore Technologies MinION sequencer, methylation calling and downstream analyses were performed as detailed in the Supplementary Methods.

Analysis of sRNAs associated with nuclear AGO1.

Raw sequencing reads of AGO1-associated RNAs from 10-day-old Col-0 at 1 hr after treatment with 50 µM MeJA or control solution, were downloaded from the NCBI Sequence Read Archive (SRR5313815 and SRR5313816). For full details of the experimental design and sequencing, see Liu et al.[44] and for details of downstream analysis conducted in this study, refer to the Supplementary Methods.

Analysis of sequence homology between *ATREP2* TEs and IR-related genes.

Genomic sequences of *ATREP2*, *ATREP7* and *TNAT1A* TEs were queried against gene sets (IR-genes, random genes or stably expressed genes) using BLAST+ v2.11.0[45] as detailed in the Supplementary Methods.

655 **Statistical analyses.**

656 Statistical analysis of bioassay data, hyperspectral imaging results, glucosinolate profiles,
657 and RT-qPCR data was conducted using R v3.6.1, as detailed in the Supplementary
658 Methods.

DATA AVAILABILITY

The mRNA-seq, WGBS and Nanopore sequencing data discussed in this publication have been deposited in NCBI's Gene Expression Omnibus and are accessible through GEO SuperSeries accession number GSE163271 (https://www.ncbi.nlm.nih.gov/geo/query/acc.cgi?acc=GSE163271). The sRNA-seq data analysed in this study was downloaded from the NCBI Sequence Read Archive (https://www.ncbi.nlm.nih.gov/sra; SRR5313815 and SRR5313816). Arabidopsis genome sequence and annotation data was downloaded from TAIR (www.arabidopsis.org) and Ensembl Plants (TAIR10.40; www.plants.ensembl.org). Biological materials are available from the corresponding authors.

ACKNOWLEDGEMENTS

We thank Professor Ted Turlings for providing *Spodoptera littoralis* eggs and Professor Roberto Solano for providing the *myc2 myc3 myc4* triple mutant. We also thank Lisa Smith, Leonardo Furci, David Pascual-Pardo, Ellie Vinnicombe and David Rapley for useful discussions, assistance with experiments and rearing of *S. littoralis*. The work presented in this publication was supported by a consolidator grant (309944 “Prime-A-Plant”) and a proof-of-concept grant (824985, “ChemPrime”) from the European Research Council to J.T., a Research Leadership Award (RL-2012-042) from the Leverhulme Trust to JT, a BBSRC-IPA grant (BB/P006698/1) to J.T., a PROMOS grant (Promo158) from the German Academic Exchange Service (DAAD) and Freie Universität to A.M. and Research Council of Norway grants (249920 and 249958/F20) to P.K. and M.H.M., respectively.

AUTHOR CONTRIBUTIONS STATEMENT

S.W.W., P.K., M.H.M. and J.T. conceived the idea for the research, which was supervised by J.T. S.W.W. conducted experiments and gathered data with assistance from A.H.P., A.M., R.S.W., M.A.H., E.K.M., P.S.C.F.R., H.H., A.L.S. and M.H.M. K.H. conducted the LC-MS/MS profiling of glucosinolates with assistance from I.S.F. Data analysis was performed by S.W.W. with assistance from A.H.P., A.M., R.S.W., M.A.H., E.K.M., H.H., J.H.M.S., A.L.S., K.H. and J.T. The paper was written by S.W.W. and J.T. with comments and input from all other authors. M.H.M., P.K. and J.T. provided funding for the research.

688 **COMPETING INTERESTS STATEMENT**

689 The authors declare no competing interests.

690 **FIGURE LEGENDS**

691 **Fig. 1 | Short- and long-term effects of JA on resistance against three different biotic**
692 **stresses. a**, Experimental setup to study short- and long-term impacts of jasmonic acid (JA)
693 on biotic stress resistance in Arabidopsis (Col-0). Plants were pre-treated with water (control,
694 blue dots) or 1 mM JA (red dots) at 1 day (short-term) or 3 weeks (long-term) before stress
695 challenge. **b**, Long-term effects of seedling treatments on JA signalling activity over the 3-
696 week period. Dashed lines depict estimated expression profiles of the JA regulatory gene
697 *MYC2* and the JA marker gene *VSP2*, based on RT-qPCR analysis over four timepoints.
698 Data points represent gene expression values of biological replicates (n=2-3) relative to the
699 mean expression value of non-treated control plants at the time of seedling treatment (grey).
700 Asterisks indicate statistically significant differences between treatments at individual time-
701 points (Two-sample t-test; N.S. $p > 0.05$, ** $p < 0.01$, *** $p < 0.001$). **c**,**d**, Short- and long-
702 term effects of JA on resistance of 5-week-old plants against the herbivore *Spodoptera*
703 *littoralis* (*Sl*), hemi-biotrophic pathogen *Pseudomonas syringae* pv. *tomato* DC3000
704 *luxCDABE* (*Pst*) and necrotrophic pathogen *Plectosphaerella cucumerina* (*Pc*). Data points
705 represent weights of individual *Sl* larvae following feeding on individual plants (n=23-34),
706 mean colony forming units (cfu) of *Pst* per cm^2 of leaf tissue per plant (n=9-12) and mean
707 per plant lesion diameters by *Pc* (n=18-21). Asterisks indicate statistically significant
708 differences between pre-treatments (Two-sample t-test for *Pc* and *Pst* assays, Welch two-
709 sample t-test or Mann-Whitney test for *Sl* assays in **c** and **d**, respectively; *** $p < 0.001$). **e**,
710 Long-term effects of JA seedling treatment on the expression of defence marker genes upon
711 challenge with either water (mock) or, 0.1 mM JA (*VSP2*), 0.5 mM salicylic acid (SA; *PR1*) or
712 0.1 mM JA + 0.1 mM 1-aminocyclopropanecarboxylic acid (ACC; *PDF1.2*). Samples for RT-
713 qPCR analysis were collected at 4, 8 and 24 hours (hrs) after challenge. Data points
714 represent gene expression values of individual replicates (n=2-4) relative to the mean
715 expression values of control plants from water-treated seedlings at 4 hrs post water
716 challenge. Seedling treatment, challenge treatment and harvest timepoint combinations

717 which do not share the same letter are significantly different (Kruskal-Wallis test followed by
718 pairwise Wilcoxon rank sum tests for *VSP2* or ANOVA followed by Tukey post-hoc test for
719 *PDF1.2* and *PR1*; *p.adj* < 0.05). Lower, middle and upper horizontal lines in boxplots indicate
720 the 1st, 2nd and 3rd quartiles; whiskers extend to the lowest and highest data points within 1.5
721 × interquartile range below and above the 1st and 3rd quartiles.

Fig. 2 | Transcriptome of long-term JA-IR against herbivory and JA-IS against pathogens. a,b, Principal component analysis (PCA) and hierarchical cluster analysis (HCA) of global gene expression patterns, respectively. Samples for mRNA-sequencing were collected from 5-week-old plants at 4 hrs after challenge with water (W) or 0.1 mM JA. Plants had been pre-treated with water or 1 mM JA at the seedling stage (2-weeks-old). Letters before and after the underscore in the heatmap labels indicate seedling treatment and challenge treatment, respectively. The darker the colour in the heatmap the higher the similarity between samples. **c**, Transcript profiles of 203, 796 and 144 genes correlating with long-term JA-IR to *Sl*, JA-IS to *Pst* and JA-IS to *Pc*, respectively. Gene clusters were selected based on expression profile and enrichment of biologically relevant GO terms. For details, see Supplementary Methods, Supplementary Fig. 1 and Extended Data Fig. 2. Blue and red columns above the heatmaps indicate water and JA treatments, respectively, of seedlings (ST) and 5-week-old plants (Challenge). Heatmap-projected values represent per gene z-scores of transformed read counts from 4 biological replicates for each treatment combination. **d**, Selection of defence-related Gene Ontology (GO) terms enriched within the sets of IR- or IS-related genes ($p.adj < 0.05$). For a complete lists of all enriched GO terms, see Supplementary Data 5, 9 and 13.

Fig. 3 | MYC2/3/4 transcription factors control short- and long-term JA-IR against herbivory. a, Statistical enrichment of transcription factor (TF) DNA binding motifs ($p < 0.01$) in the 1 kb upstream promoter sequences of the 203 IR-related genes (Fig. 2c). Displayed are the 8 motifs with the strongest statistical enrichment. Enrichment breadth indicates the % of promoters for which the motif fell within the top 5% of most strongly enriched motifs. Name and ID indicate predicted TF binding to the DNA motif. For the complete list of all statistically enriched DNA motifs, see Supplementary Data 14. **b**, Short- and long-term effects of water (blue) and 1 mM JA (red) pre-treatment on resistance of 5-week-old WT (Col-0) and *myc2 myc3 myc4* (*mycT*) plants against herbivory by *Spodoptera littoralis* (*Sl*; n=23-24). Pre-treatment and genotype combinations which do not share the same letter are significantly different (Kruskal-Wallis test followed by pairwise Wilcoxon rank sum tests for the short-term IR assay; ANOVA followed by Tukey post-hoc test for the long-term IR assay; $p.adj < 0.05$). For more details, see legend to Fig. 1c,d.

Fig. 4 | Long-term JA-IR against herbivory and associated shifts in glucosinolate profiles require intact DNA methylation homeostasis. a,**b,** Short- (**a**) and long-term (**b**) effects of water (blue) and 1 mM JA (red) pre-treatment on resistance of 5-week-old WT (Col-0) and RdDM (*nrpe1-11*) and ROS1 (*ros1-4*) mutant plants against herbivory by *Spodoptera littoralis* (*Sl*, *n*=23-24). If the pre-treatment (PT) or seedling treatment (ST) x Genotype (G) interaction term was significant (Two-way ANOVA, $p < 0.05$), a Tukey post-doc test was conducted with different letters indicating significant differences between means ($p < 0.05$). For more details, see legend to Fig. 1. **c**, Effects of long-term JA-IR on attractiveness to *Sl* larvae in dual-choice tests. Shown are the number of larvae preferring 5-week-old plants pre-treated with either water (blue) or 1 mM JA (red) at the seedling stage (2-week-old). White boxes indicate larvae failing to make a choice. Asterisks indicate statistically uneven distributions of larval numbers between treatments (Goodness-of-fit test, * $p < 0.05$). **d**, Long-term effects of seeding treatment with water or 1 mM JA on all glucosinolates in leaves of 5-week-old WT and *ros1-4* plants. Heatmap-projected values represent per metabolite z-scores of concentrations (µg/g dry mass) from 8 biological replicates for each genotype-treatment combination. See Extended Data Fig. 4 for raw data. Asterisks indicate significant effects of ST, G or ST x G (Two-way ANOVA, * = $p < 0.05$, ** = $p < 0.01$, *** = $p < 0.001$). **e**, Biosynthesis pathways of indole (top) and aliphatic (bottom) glucosinolates. Heatmap-project values represent z-scores of mean concentrations (µg/g dry mass). CW: Col-0 + water ST, CJ: Col-0 + JA ST, rW: *ros1-4* + water ST, rJ: *ros1-4* + JA ST, nd: not detected, I3M: glucobrassicin, 1OHI3M: 1-hydroxyglucobrassicin, 4OHI3M: 4-hydroxyglucobrassicin, 4MOI3M: 4-methoxyglucobrassicin, NMOI3M: neoglucobrassicin, 3mtp: 3-methylthiopropyl glucosinolate, 3msp: glucoiberin, 4mtb: glucoerucin, 4msb: glucoraphanin.

Fig. 5 | The DNA methylome of long-term JA-IR is associated with selective hypomethylation of *ATREP2* transposable elements. Biologically replicated leaf samples (*n*=3) for whole-genome bisulphite sequencing were collected from 5-week-old plants treated with water or 1 mM JA at the seedling stage (2-week-old). **a**, PCA plot displaying variation in global DNA methylation at all sequence contexts (all-C) between samples from water (blue) and JA (red) treated plants. **b**, HCA plots displaying global variation in DNA methylation at all-C, CG, CHG and CHH contexts (C is cytosine and H is any nucleotide other than G). **c**, Numbers of differentially methylated regions (DMRs) between individual samples from JA-treated plants (JA.1, JA.2 and JA.3) and all three samples from water-treated plants (1JA_vs_3W comparisons) at gene promoters, exons, introns and intergenic regions. Frequencies of hyper- and hypo-methylated DMRs are indicated by the bars above and below the x-axis, respectively. DMRs at transposable elements (TE) are indicated by dark shading. **d**,**e**, Enrichment of TE families amongst the TEs overlapped by DMRs at all-C and CHH contexts, respectively. Graphs plot statistical significance of enrichment for each TE family against corresponding fold-enrichment, represented by mean $-\log_{10}$(*p.adj*) values (± SEM) and mean fold enrichment values (± SEM), respectively. Enrichment is expressed relative to the background of all genome-annotated TEs (TAIR v10). Labelled data points indicate TE families with a mean $-\log_{10}$(*p.adj*) > $-\log_{10}(0.05)$ (**d**) or $-\log_{10}(0.001)$ (**e**). Brightly coloured data points indicate TE families that were significantly overrepresented in 1 (red), 2 (yellow) or 3 (green) comparisons, respectively (*p.adj* ≤ 0.05). The red dashed line is at $-\log_{10}(0.05)$.

Fig. 6 | Role of *ATREP2* TEs, DNA (de)methylation pathways, and AGO1 in long-term JA-IR against herbivory. a, Average DNA methylation (all-C context) in TEs from the *ATREP2* family relative to TEs from two similarly sized class-2 families that were not enriched with JA-induced hypomethylation (*ATREP7* and *TNAT1A*). Shown are percentages of DNA methylation for each TE family in leaves of Col-0 (WT), *nrpe1-11* (RdDM mutant) and *ros1-4*. *n* indicates the number of TEs with sufficient coverage across all genotypes for inclusion in the analysis (≥ 5 reads for ≥ 50 % of cytosines). **b**, Impact of ectopic induction of recombinant ROS1-YFP on average DNA methylation (all-C context) of *ATREP2*, *ATREP7* and *TNAT1A* TEs in transgenic *XVE:ROS1-YFP* plants. Violin plots show the difference in DNA methylation between DMSO-treated control plants and estradiol-treated plants; *n* indicates the number of TEs with sufficient coverage across both treatments for inclusion in the analysis (≥ 5 reads for ≥ 50 % of cytosines). Asterisks indicate statistically significant reductions in methylation levels (One-sample one-tailed t-test; * $p < 1 \times 10^{-10}$). **c**, Histograms of sequence alignments between *ATREP2*, *ATREP7* and *TNAT1A* TEs and protein-coding genes. Top panels show alignments with the gene bodies (left) and 1 kb promoters of the 203 IR-related genes. As extra controls, the middle and bottom panels show similar alignments for 203 randomly selected genes (Random) or 203 stably expressed genes (Stably expr)[67], respectively. Crosses indicate the number of unique genes with alignments to a particular TE family in a particular bin (right y-axis). Alignments were filtered by length (≥ 19 nt and ≤ 300 nt) and expect value (e < 0.05). Alignments with genes overlapping with TEs from the family of interest were removed. **d**, Long-term effects of seedling treatment with water (blue) and 1 mM JA (red) on resistance of 5-week-old WT (Col-0) and *ago1* plants against herbivory by *Spodoptera littoralis* (*Sl*, *n*=15-18). For details, see legend to Fig. 1. As the seedling treatment (ST) x Genotype (G) interaction term was significant (Two-way ANOVA, $p < 0.05$), a Tukey post-doc test was conducted with different letters indicating statistically significant differences between treatment-genotype combinations ($p < 0.05$). **e**, Hypothetical model of the elicitation, maintenance, and expression of long-term JA-IR against herbivory. (1) Naïve state: seedlings exhibit high levels of DNA methylation at

825 *ATREP2* TEs which is regulated by RdDM. (2) Elicitation: JA treatment of 2-week-old
826 seedlings elicits MYC-dependent induction of JA defence genes (basal induction) and
827 stochastic hypomethylation of *ATREP2* TEs by ROS1. (3) Maintenance: hypomethylated
828 *ATREP2* TEs are released from silencing, resulting in the production of transcripts that are
829 cleaved by post-transcriptional gene silencing (PTGS) into 21-22 nt siRNAs (short green
830 lines) that associate with AGO1 and drive the initiation phase of RdDM. Due to sequence
831 homology, siRNAs guide AGO1 to JA defence genes (dashed black line), where it mediates
832 euchromatisation to weakly upregulate/prime JA defence genes. (4) Expression: the AGO1-
833 mediated changes in chromatin enable augmented induction of JA defence genes by MYC
834 transcription factors upon challenge by a JA-inducing stress (e.g. *Sl* herbivory).

REFERENCES

1. Wilkinson, S. W. *et al.* Surviving in a hostile world: plant strategies to resist pests and diseases. *Annu. Rev. Phytopathol.* **57**, 505–529 (2019).

2. Irieda, H. *et al.* Conserved fungal effector suppresses PAMP-triggered immunity by targeting plant immune kinases. *Proc. Natl. Acad. Sci. U. S. A.* **116**, 496–505 (2019).

3. Erb, M. & Reymond, P. Molecular interactions between plants and insect herbivores. *Annu. Rev. Plant Biol.* **70**, 527–557 (2019).

4. Pel, M. J. C. & Pieterse, C. M. J. Microbial recognition and evasion of host immunity. *J. Exp. Bot.* **64**, 1237–1248 (2013).

5. Ahmad, S., Gordon-Weeks, R., Pickett, J. & Ton, J. Natural variation in priming of basal resistance: from evolutionary origin to agricultural exploitation. *Mol. Plant Pathol.* **11**, 817–827 (2010).

6. Bigeard, J., Colcombet, J. & Hirt, H. Signaling mechanisms in pattern-triggered immunity (PTI). *Mol. Plant* **8**, 521–539 (2015).

7. Pieterse, C. M. J., Van der Does, D., Zamioudis, C., Leon-Reyes, A. & Van Wees, S. C. M. Hormonal modulation of plant immunity. *Annu. Rev. Cell Dev. Biol.* **28**, 489–521 (2012).

8. Glazebrook, J. Contrasting mechanisms of defense against biotrophic and necrotrophic pathogens. *Annu. Rev. Phytopathol.* **43**, 205–227 (2005).

9. Thines, B. *et al.* JAZ repressor proteins are targets of the SCF^{COI1} complex during jasmonate signalling. *Nature* **448**, 661–665 (2007).

10. Sheard, L. B. *et al.* Jasmonate perception by inositol-phosphate-potentiated COI1-JAZ co-receptor. *Nature* **468**, 400–407 (2010).

11. Howe, G. A., Major, I. T. & Koo, A. J. Modularity in jasmonate signaling for multistress

resilience. *Annu. Rev. Plant Biol.* **69**, 387–415 (2018).

12. Chini, A., Gimenez-Ibanez, S., Goossens, A. & Solano, R. Redundancy and specificity in jasmonate signalling. *Curr. Opin. Plant Biol.* **33**, 147–156 (2016).

13. Zhu, Z. *et al.* Derepression of ethylene-stabilized transcription factors (EIN3/EIL1) mediates jasmonate and ethylene signaling synergy in *Arabidopsis*. *Proc. Natl. Acad. Sci. U. S. A.* **108**, 12539–12544 (2011).

14. Chini, A. *et al.* The JAZ family of repressors is the missing link in jasmonate signalling. *Nature* **448**, 666–671 (2007).

15. Anderson, J. P. *et al.* Antagonistic interaction between abscisic acid and jasmonate-ethylene signaling pathways modulates defense gene expression and disease resistance in Arabidopsis. *Plant Cell* **16**, 3460–3479 (2004).

16. Bodenhausen, N. & Reymond, P. Signaling pathways controlling induced resistance to insect herbivores in *Arabidopsis*. *Mol. Plant-Microbe Interact. MPMI* **20**, 1406–1420 (2007).

17. Fernández-Calvo, P. *et al.* The *Arabidopsis* bHLH transcription factors MYC3 and MYC4 are targets of JAZ repressors and act additively with MYC2 in the activation of jasmonate responses. *Plant Cell* **23**, 701–715 (2011).

18. Song, S. *et al.* Interaction between MYC2 and ETHYLENE INSENSITIVE3 modulates antagonism between jasmonate and ethylene signaling in *Arabidopsis*. *Plant Cell* **26**, 263–279 (2014).

19. Rasmann, S. *et al.* Herbivory in the previous generation primes plants for enhanced insect resistance. *Plant Physiol.* **158**, 854–863 (2012).

20. Zhang, H., Lang, Z. & Zhu, J. K. Dynamics and function of DNA methylation in plants. *Nat. Rev. Mol. Cell Biol.* **19**, 489–506 (2018).

21. Matzke, M. A. & Mosher, R. A. RNA-directed DNA methylation: an epigenetic pathway of increasing complexity. *Nat. Rev. Genet.* **15**, 394–408 (2014).

22. Cuerda-Gil, D. & Slotkin, R. K. Non-canonical RNA-directed DNA methylation. *Nat. Plants* **2**, 16163 (2016).

23. Tang, K., Lang, Z., Zhang, H. & Zhu, J. K. The DNA demethylase ROS1 targets genomic regions with distinct chromatin modification. *Nat. Plants* **2**, 16169 (2016).

24. Sigman, M. J. *et al.* An siRNA-guided ARGONAUTE protein directs RNA polymerase V to initiate DNA methylation. *Nat. Plants* **7**, 1461–1474 (2021).

25. Yu, A. *et al.* Dynamics and biological relevance of DNA demethylation in *Arabidopsis* antibacterial defense. *Proc. Natl. Acad. Sci. U. S. A.* **110**, 2389–2394 (2013).

26. López Sánchez, A., Stassen, J. H. M., Furci, L., Smith, L. M. & Ton, J. The role of DNA (de)methylation in immune responsiveness of Arabidopsis. *Plant J.* **88**, 361–374 (2016).

27. Halter, T. *et al.* The Arabidopsis active demethylase ROS1 *cis*-regulates defence genes by erasing DNA methylation at promoter-regulatory regions. *Elife* **10**, e62994 (2021).

28. Cui, J. *et al. Pseudomonas syringae* manipulates systemic plant defenses against pathogens and herbivores. *Proc. Natl. Acad. Sci. U. S. A.* **102**, 1791–1796 (2005).

29. Murmu, J. *et al. Arabidopsis* GOLDEN2-LIKE (GLK) transcription factors activate jasmonic acid (JA)-dependent disease susceptibility to the biotrophic pathogen *Hyaloperonospora arabidopsidis*, as well as JA-independent plant immunity against the necrotrophic pathogen *Botrytis cinerea*. *Mol. Plant Pathol.* **15**, 174–184 (2014).

30. Scholz, S. S. *et al.* Mutation of the *Arabidopsis* calmodulin-like protein CML37 deregulates the jasmonate pathway and enhances susceptibility to herbivory. *Mol. Plant* **7**, 1712–1726 (2014).

908 31. Hickman, R. *et al.* Architecture and dynamics of the jasmonic acid gene regulatory
909 network. *Plant Cell* **29**, 2086–2105 (2017).

910 32. Lian, T. fei, Xu, Y. ping, Li, L. fen & Su, X. D. Crystal structure of tetrameric
911 *Arabidopsis* MYC2 reveals the mechanism of enhanced interaction with DNA. *Cell*
912 *Rep.* **19**, 1334–1342 (2017).

913 33. Carretero-Paulet, L. *et al.* Genome-wide classification and evolutionary analysis of the
914 bHLH family of transcription factors in Arabidopsis, poplar, rice, moss, and algae.
915 *Plant Physiol.* **153**, 1398–1412 (2010).

916 34. Schweizer, F. *et al. Arabidopsis* basic helix-loop-helix transcription factors MYC2,
917 MYC3, and MYC4 regulate glucosinolate biosynthesis, insect performance, and
918 feeding behavior. *Plant Cell* **25**, 3117–3132 (2013).

919 35. Law, J. A. & Jacobsen, S. E. Establishing, maintaining and modifying DNA
920 methylation patterns in plants and animals. *Nat. Rev. Genet.* **11**, 204–220 (2010).

921 36. Furci, L. *et al.* Identification and characterisation of hypomethylated DNA loci
922 controlling quantitative resistance in *Arabidopsis*. *Elife* **8**, e40655 (2019).

923 37. Niederhuth, C. E. *et al.* Widespread natural variation of DNA methylation within
924 angiosperms. *Genome Biol.* **17**, 194 (2016).

925 38. Cokus, S. J. *et al.* Shotgun bisulphite sequencing of the *Arabidopsis* genome reveals
926 DNA methylation patterning. *Nature* **452**, 215–219 (2008).

927 39. O'Malley, R. C. *et al.* Cistrome and Epicistrome features shape the regulatory DNA
928 landscape. *Cell* **165**, 1280–1292 (2016).

929 40. Williams, B. P., Pignatta, D., Henikoff, S. & Gehring, M. Methylation-sensitive
930 expression of a DNA demethylase gene serves as an epigenetic rheostat. *PLoS*
931 *Genet.* **11**, e1005142 (2015).

41. Gallego-Bartolomé, J. *et al.* Targeted DNA demethylation of the *Arabidopsis* genome using the human TET1 catalytic domain. *Proc. Natl. Acad. Sci. U. S. A.* **115**, E2125–E2134 (2018).

42. Cambiagno, D. A. *et al.* Immune receptor genes and pericentromeric transposons as targets of common epigenetic regulatory elements. *Plant J.* **96**, 1178–1190 (2018).

43. Wicker, T. *et al.* A unified classification system for eukaryotic transposable elements. *Nat. Rev. Genet.* **8**, 973–982 (2007).

44. Liu, C. *et al. Arabidopsis* ARGONAUTE 1 binds chromatin to promote gene transcription in response to hormones and stresses. *Dev. Cell* **44**, 348–361 (2018).

45. Camacho, C. *et al.* BLAST+: architecture and applications. *BMC Bioinformatics* **10**, 421 (2009).

46. Smith, M. R. *et al.* Cyclophilin 40 is required for microRNA activity in *Arabidopsis*. *Proc. Natl. Acad. Sci. U. S. A.* **106**, 5424–5429 (2009).

47. Wasternack, C. How jasmonates earned their laurels: past and present. *J. Plant Growth Regul.* **34**, 761–794 (2015).

48. Liu, Y. *et al.* Arabidopsis vegetative storage protein is an anti-insect acid phosphatase. *Plant Physiol.* **139**, 1545–1556 (2005).

49. Parker, A. H., Wilkinson, S. W. & Ton, J. Epigenetics: a catalyst of plant immunity against pathogens. *New Phytol.* **233**, 66–83 (2022).

50. Deleris, A., Halter, T. & Navarro, L. DNA methylation and Demethylation in plant immunity. *Annu. Rev. Phytopathol.* **54**, 579–603 (2016).

51. Dowen, R. H. *et al.* Widespread dynamic DNA methylation in response to biotic stress. *Proc. Natl. Acad. Sci. U. S. A.* **109**, E2183–E2191 (2012).

52. Pavet, V., Quintero, C., Cecchini, N. M., Rosa, A. L. & Alvarez, M. E. *Arabidopsis*

displays centromeric DNA hypomethylation and cytological alterations of heterochromatin upon attack by *Pseudomonas syringae*. *Mol. Plant-Microbe Interact.* **19**, 577–587 (2006).

53. Kellenberger, R. T., Schlüter, P. M. & Schiestl, F. P. Herbivore-Induced DNA demethylation changes floral signalling and attractiveness to pollinators in *Brassica rapa*. *PLoS One* **11**, e0166646 (2016).

54. Atighi, M. R., Verstraeten, B., De Meyer, T. & Kyndt, T. Genome-wide DNA hypomethylation shapes nematode pattern-triggered immunity in plants. *New Phytol.* **227**, 545–558 (2020).

55. Hewezi, T. *et al.* Cyst nematode parasitism induces dynamic changes in the root epigenome. *Plant Physiol.* **174**, 405–420 (2017).

56. Garrigues, J. M., Tsu, B. V., Daugherty, M. D. & Pasquinelli, A. E. Diversification of the *Caenorhabditis* heat shock response by Helitron transposable elements. *Elife* **8**, e51139 (2019).

57. Quesneville, H. Twenty years of transposable element analysis in the *Arabidopsis thaliana* genome. *Mob. DNA* **11**, 28 (2020).

58. Tanurdzic, M. *et al.* Epigenomic consequences of immortalized plant cell suspension culture. *PLOS Biol.* **6**, e302 (2008).

59. Panda, K. & Slotkin, R. K. Long-read cDNA sequencing enables a ‘Gene-Like’ transcript annotation of transposable elements. *Plant Cell* **32**, 2687–2698 (2020).

60. Fan, J., Crooks, C. & Lamb, C. High-throughput quantitative luminescence assay of the growth in planta of *Pseudomonas syringae* chromosomally tagged with *Photorhabdus luminescens luxCDABE*. *Plant J.* **53**, 393–399 (2008).

61. Ton, J. & Mauch-Mani, B. β-amino-butyric acid-induced resistance against necrotrophic pathogens is based on ABA-dependent priming for callose. *Plant J.* **38**,

119–130 (2004).

62. Pétriacq, P., Stassen, J. & Ton, J. Spore density determines infection strategy by the plant-pathogenic fungus *Plectosphaerella cucumerina*. *Plant Physiol.* **170**, 2325–2339 (2016).

63. Yang, L. *et al.* Salicylic acid biosynthesis is enhanced and contributes to increased biotrophic pathogen resistance in *Arabidopsis* hybrids. *Nat. Commun.* **6**, 7309 (2015).

64. Siligato, R. *et al.* Multisite gateway-compatible cell type-specific gene-inducible system for plants. *Plant Physiol.* **170**, 627–641 (2016).

65. Zuo, J., Niu, Q. W. & Chua, N. H. An estrogen receptor-based transactivator XVE mediates highly inducible gene expression in transgenic plants. *Plant J.* **24**, 265–273 (2000).

66. Hooshmand, K. & Fomsgaard, I. S. Analytical Methods for Quantification and Identification of Intact Glucosinolates in Arabidopsis Roots Using LC-QqQ(LIT)-MS/MS. *Metabolites* **11**, 47 (2021).

67. Czechowski, T., Stitt, M., Altmann, T., Udvardi, M. K. & Scheible, W. R. Genome-wide identification and testing of superior reference genes for transcript normalization in Arabidopsis. *Plant Physiol.* **139**, 5–17 (2005).

68. Gupta, G. P., Rani, S., Birah, A. & Raghuraman, M. Improved artificial diet for mass rearing of the tobacco caterpillar, *Spodoptera litura* (Lepidoptera: Noctuidae). *Int. J. Trop. Insect Sci.* **25**, 55–58 (2005).

69. Roeder, K. A., Kuriachan, I., Vinson, S. B. & Behmer, S. T. Evaluation of a microbial inhibitor in artificial diets of a generalist caterpillar, *Heliothis virescens*. *J. Insect Sci.* **10**, 197 (2010).

70. Bricchi, I. *et al.* Separation of early and late responses to herbivory in Arabidopsis by changing plasmodesmal function. *Plant J.* **73**, 14–25 (2013).

1006 71. Brunel, D. An alternative, rapid method of plant DNA extraction for PCR analyses.
1007 *Nucleic Acids Res.* **20**, 4676 (1992).

1008 72. Harrison, S. J. *et al.* A rapid and robust method of identifying transformed *Arabidopsis*
1009 thaliana seedlings following floral dip transformation. *Plant Methods* **2**, 19 (2006).

1010 73. Ewels, P., Magnusson, M., Lundin, S. & Käller, M. MultiQC: summarize analysis
1011 results for multiple tools and samples in a single report. *Bioinformatics* **32**, 3047–3048
1012 (2016).

1013 74. Bolger, A. M., Lohse, M. & Usadel, B. Trimmomatic: a flexible trimmer for Illumina
1014 sequence data. *Bioinformatics* **30**, 2114–2120 (2014).

1015 75. Dobin, A. *et al.* STAR: ultrafast universal RNA-seq aligner. *Bioinformatics* **29**, 15–21
1016 (2013).

1017 76. Anders, S., Pyl, P. T. & Huber, W. HTSeq - a Python framework to work with high-
1018 throughput sequencing data. *Bioinformatics* **31**, 166–169 (2015).

1019 77. Anders, S. & Huber, W. Differential expression analysis for sequence count data.
1020 *Genome Biol.* **11**, R106 (2010).

1021 78. Love, M. I., Huber, W. & Anders, S. Moderated estimation of fold change and
1022 dispersion for RNA-seq data with DESeq2. *Genome Biol.* **15**, 550 (2014).

1023 79. Krueger, F. & Andrews, S. R. Bismark: a flexible aligner and methylation caller for
1024 Bisulfite-Seq applications. *Bioinformatics* **27**, 1571–1572 (2011).

1025 80. Langmead, B. & Salzberg, S. L. Fast gapped-read alignment with Bowtie 2. *Nat.*
1026 *Methods* **9**, 357–359 (2012).

1027 81. Li, H. *et al.* The Sequence Alignment/Map format and SAMtools. *Bioinformatics* **25**,
1028 2078–2079 (2009).

1029 82. Stuart, T., Buckberry, S. & Lister, R. Approaches for the analysis and interpretation of

whole genome bisulfite sequencing data. in *Epigenome Editing: Methods and Protocols, Methods in Molecular Biology* (eds. Jeltsch, A. & Rots, M. G.) 299–310 (Humana Press, 2018).

83. Schultz, M. D., Schmitz, R. J. & Ecker, J. R. 'Leveling' the playing field for analyses of single-base resolution DNA methylomes. *Trends Genet.* **28**, 583–585 (2012).

84. Feng, H., Conneely, K. N. & Wu, H. A Bayesian hierarchical model to detect differentially methylated loci from single nucleotide resolution sequencing data. *Nucleic Acids Res.* **42**, e69 (2014).

85. Wu, H. *et al.* Detection of differentially methylated regions from whole-genome bisulfite sequencing data without replicates. *Nucleic Acids Res.* **43**, e141 (2015).

86. Quinlan, A. R. & Hall, I. M. BEDTools: a flexible suite of utilities for comparing genomic features. *Bioinformatics* **26**, 841–842 (2010).

87. Ni, P. *et al.* Genome-wide detection of cytosine methylations in plant from Nanopore data using deep learning. *Nat. Commun.* **12**, 5976 (2021).

88. Thorvaldsdóttir, H., Robinson, J. T. & Mesirov, J. P. Integrative Genomics Viewer (IGV): high-performance genomics data visualization and exploration. *Brief. Bioinform.* **14**, 178–192 (2013).

89. Duan, C. G. *et al.* MET18 Connects the Cytosolic Iron-Sulfur Cluster Assembly Pathway to Active DNA Demethylation in Arabidopsis. *PLoS Genet.* **11**, e1005559 (2015).

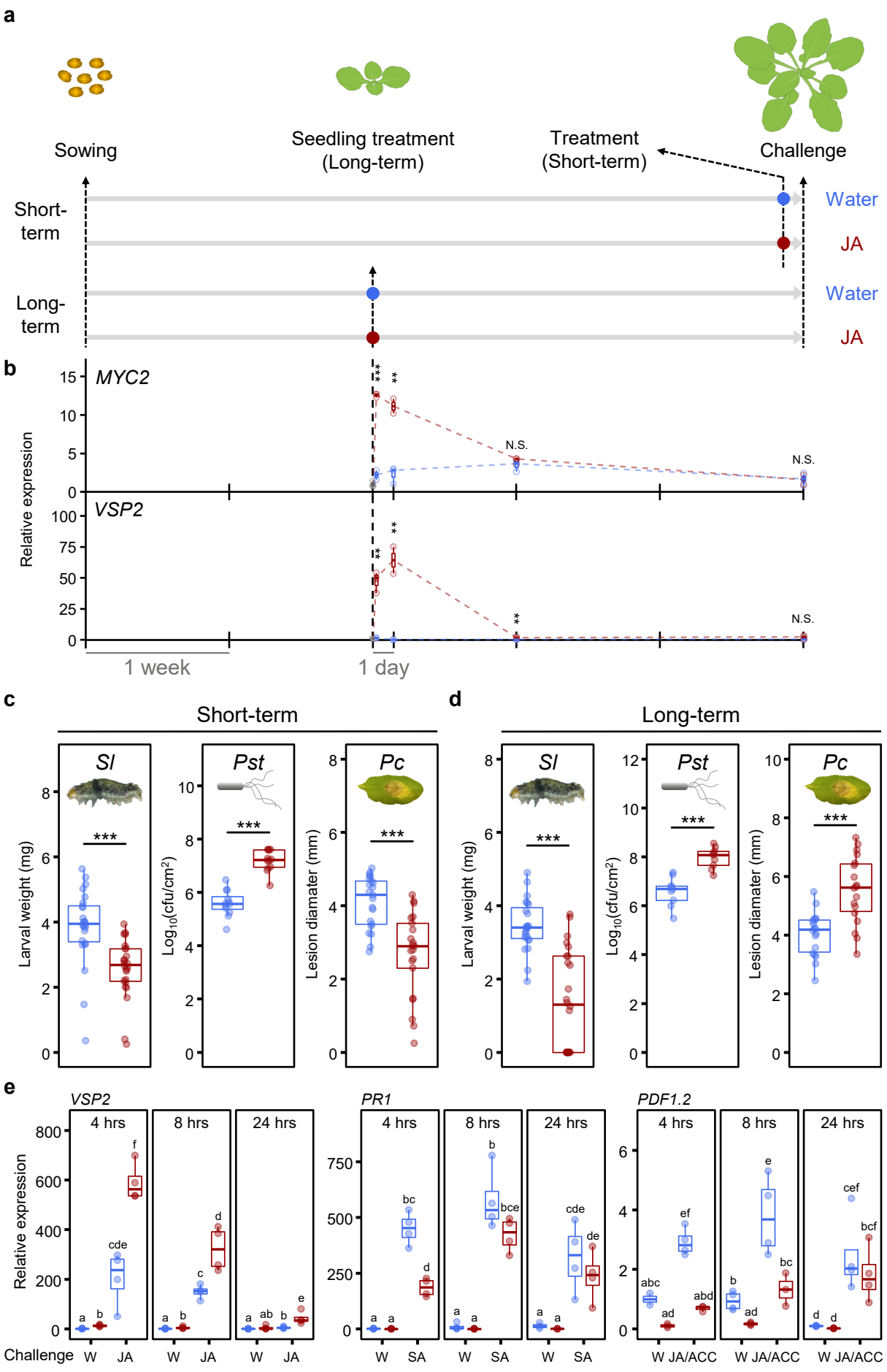
a
Sowing
Seedling treatment
(Long-term)
Treatment
(Short-term)
Challenge
Short-
term
Long-
term
Water
JA
Water
JA
b
MYC2
VSP2
Relative expression
N.S.
1 week
1 day
c
Short-term
d
Long-term
Sl
Pst
Pc
Larval weight (mg)
Log10(cfu/cm2)
Lesion diamater (mm)
e
VSP2
PR1
PDF1.2
4 hrs
8 hrs
24 hrs
Relative expression
Challenge
W
JA
SA
JA/ACC

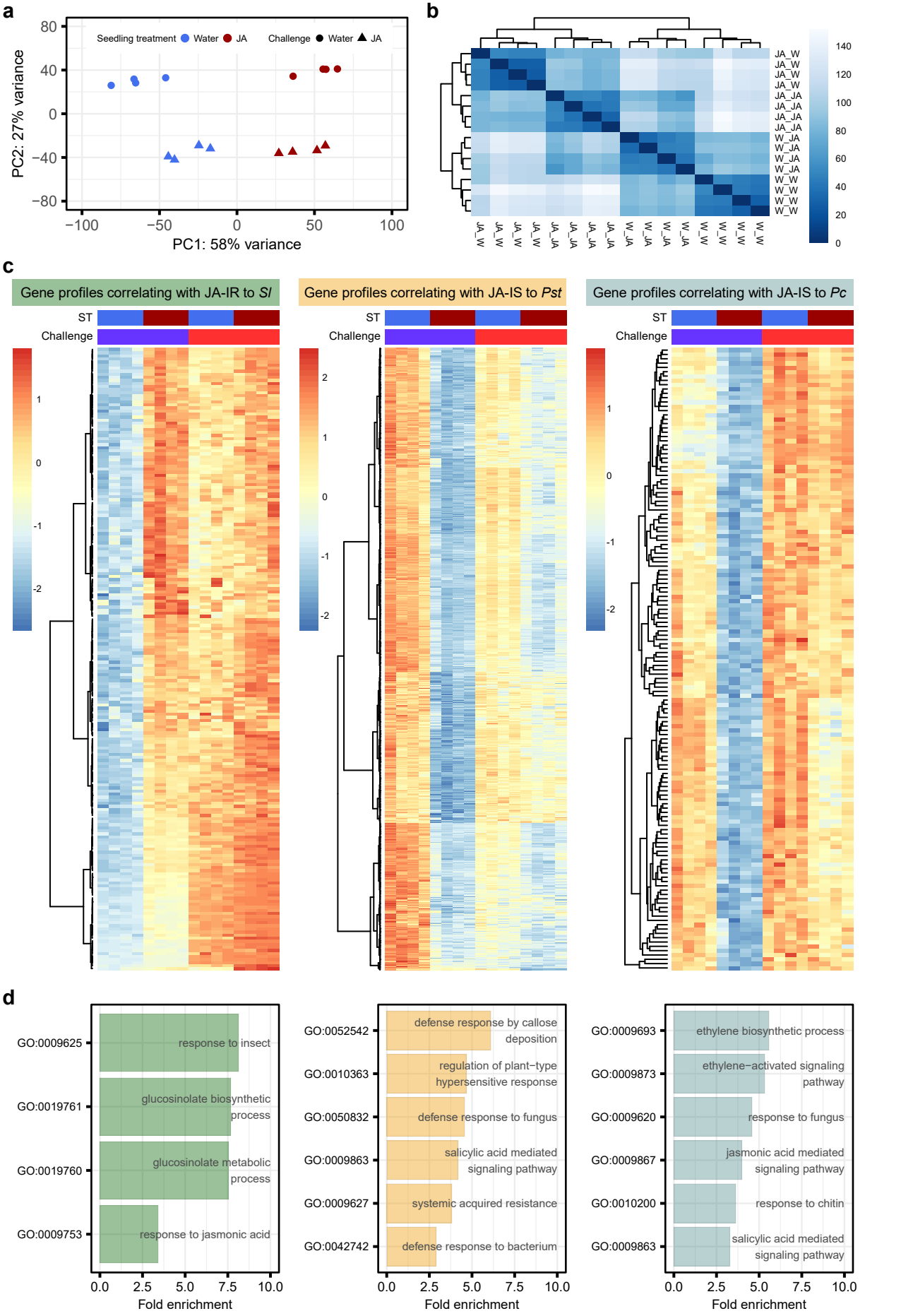
a
Seedling treatment Water JA
Challenge Water JA
PC2: 27% variance
PC1: 58% variance
b
JA_W
JA_JA
W_JA
W_W
c
Gene profiles correlating with JA-IR to SI
Gene profiles correlating with JA-IS to Pst
Gene profiles correlating with JA-IS to Pc
ST
Challenge
d
GO:0009625 response to insect
GO:0019761 glucosinolate biosynthetic process
GO:0019760 glucosinolate metabolic process
GO:0009753 response to jasmonic acid
GO:0052542 defense response by callose deposition
GO:0010363 regulation of plant−type hypersensitive response
GO:0050832 defense response to fungus
GO:0009863 salicylic acid mediated signaling pathway
GO:0009627 systemic acquired resistance
GO:0042742 defense response to bacterium
GO:0009693 ethylene biosynthetic process
GO:0009873 ethylene−activated signaling pathway
GO:0009620 response to fungus
GO:0009867 jasmonic acid mediated signaling pathway
GO:0010200 response to chitin
GO:0009863 salicylic acid mediated signaling pathway
Fold enrichment

a

Sequence Logo				
Name	PIF3	JAM2	UNE10	BPE
ID	AT1G09530	AT1G01260	AT4G00050	AT1G59640
Enrichment Breadth (%)	6.4	15.8	10.3	1.5
Sequence Logo				
Name	LHY1	MYC3	ATHB7	MYC4
ID	AT1G01060	AT5G46760	AT2G46680	AT4G17880
Enrichment Breadth (%)	14.8	9.4	5.4	3.9

b

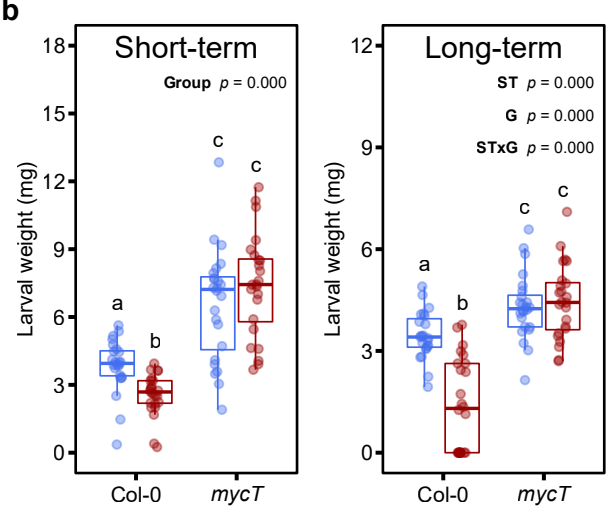

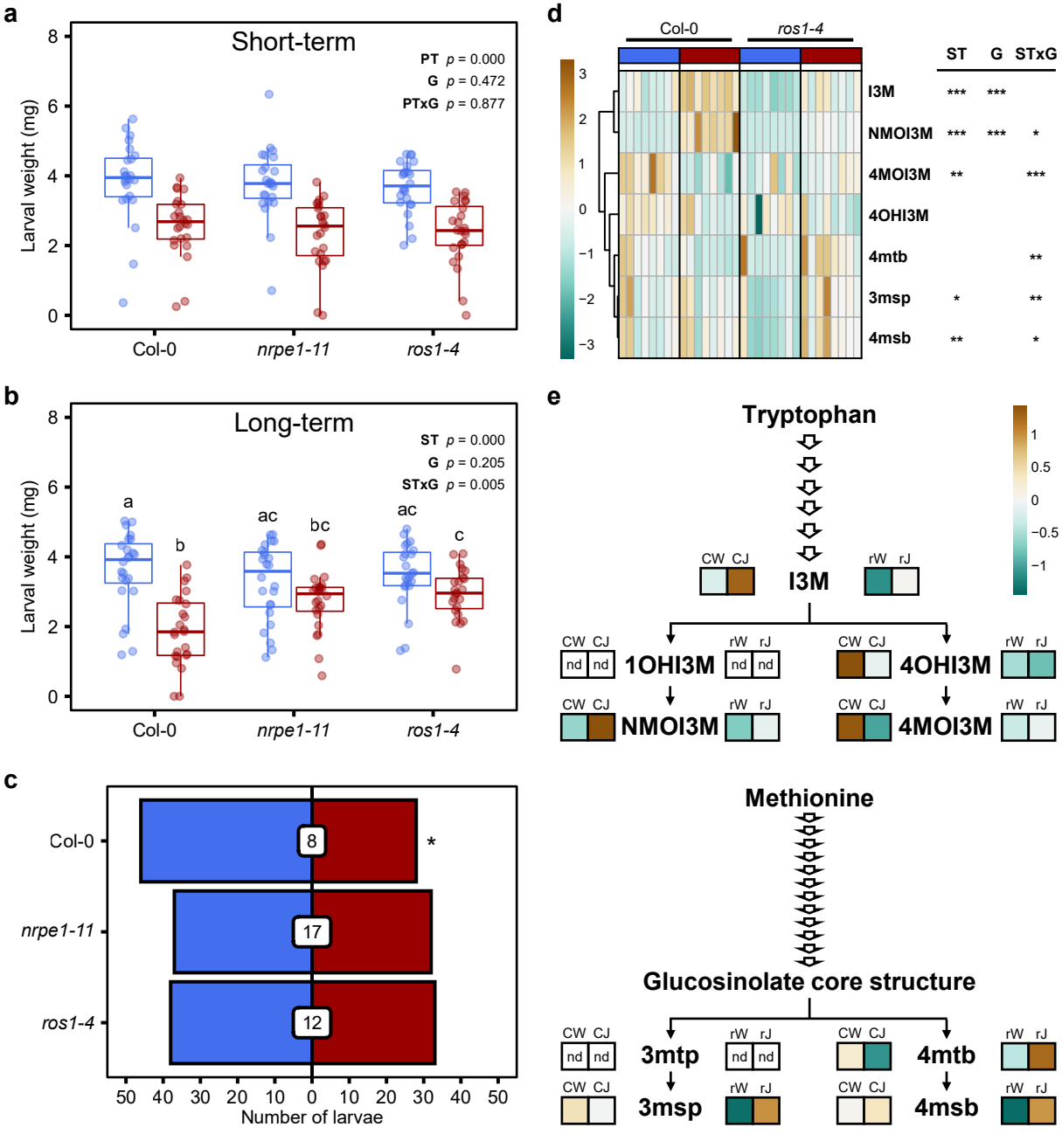
a
Short-term
PT p = 0.000
G p = 0.472
PTxG p = 0.877
Larval weight (mg)
Col-0
nrpe1-11
ros1-4
b
Long-term
ST p = 0.000
G p = 0.205
STxG p = 0.005
a
b
ac
bc
ac
c
c
8
17
12
Number of larvae
d
Col-0
ros1-4
ST G STxG
I3M *** ***
NMOI3M *** *** *
4MOI3M ** ***
4OHI3M
4mtb **
3msp * **
4msb ** *
e
Tryptophan
I3M
1OHI3M
4OHI3M
NMOI3M
4MOI3M
Methionine
Glucosinolate core structure
3mtp
4mtb
3msp
4msb
CW CJ
rW rJ
nd

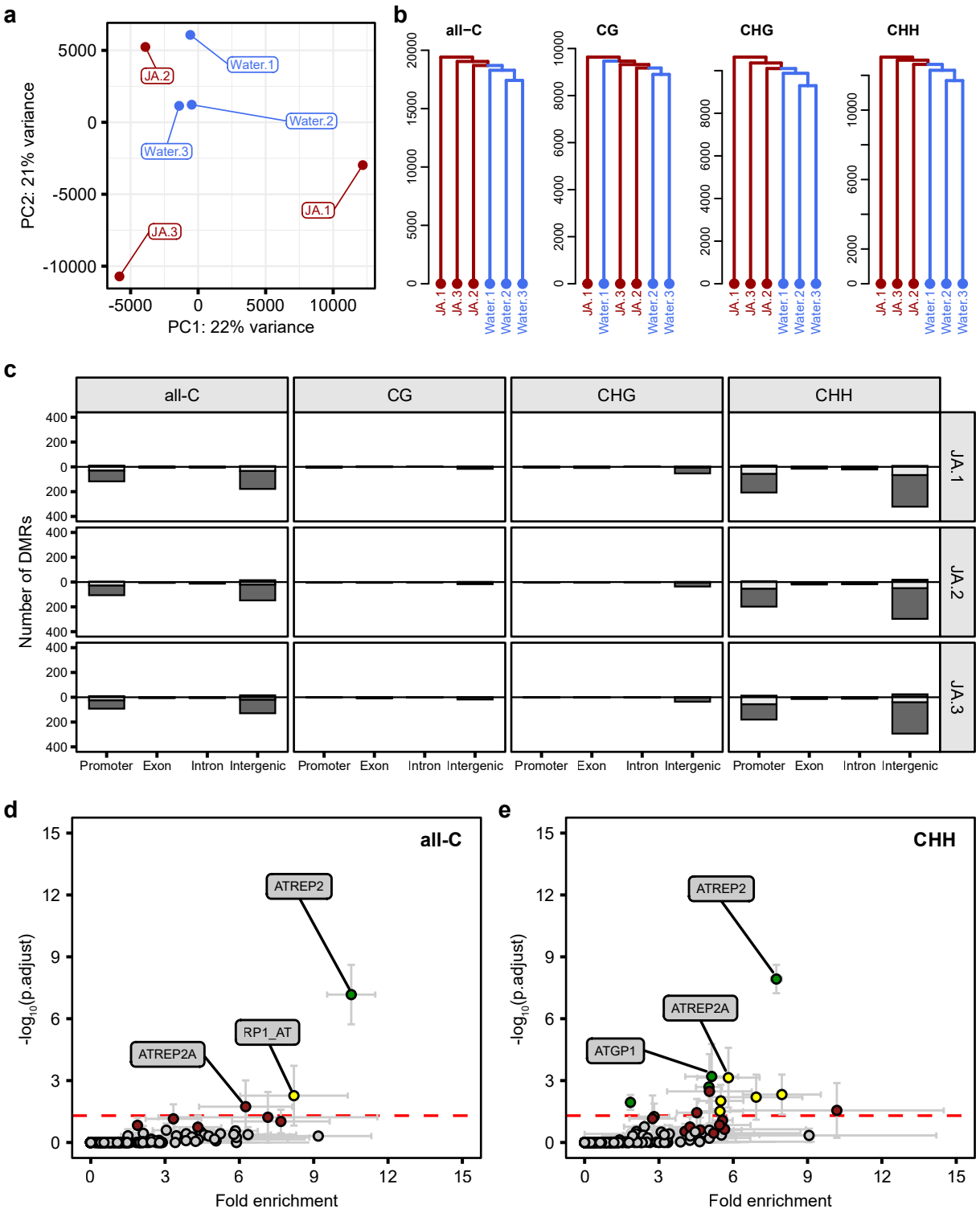
a
PC2: 21% variance
PC1: 22% variance
JA.1
JA.2
JA.3
Water.1
Water.2
Water.3
b
all−C
CG
CHG
CHH
c
Number of DMRs
Promoter
Exon
Intron
Intergenic
d
all-C
e
CHH
-log10(p.adjust)
Fold enrichment
ATREP2
ATREP2A
RP1_AT
ATGP1

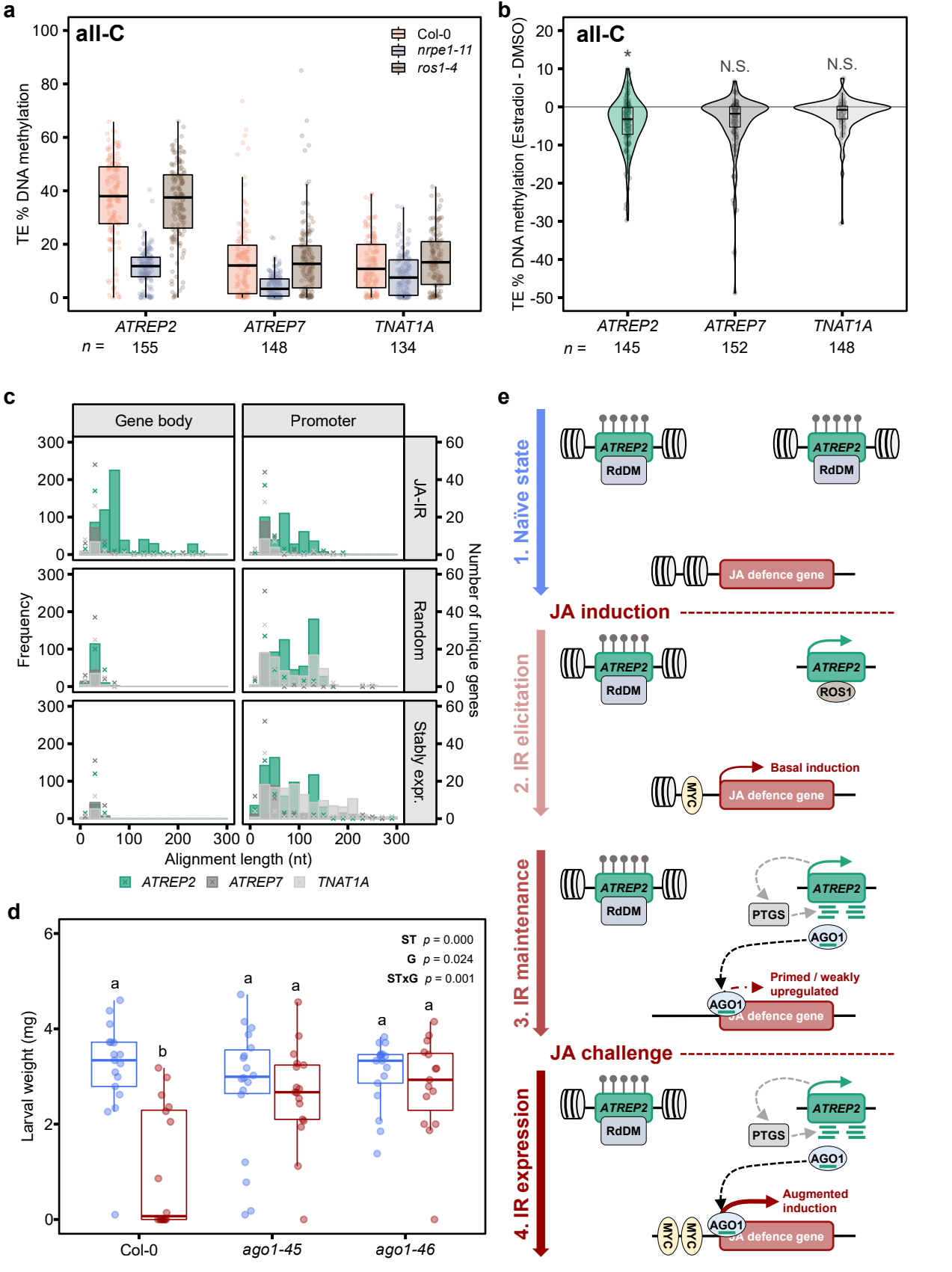
a
all-C
Col-0
nrpe1-11
ros1-4
TE % DNA methylation
ATREP2
ATREP7
TNAT1A
n = 155 148 134
b
all-C
TE % DNA methylation (Estradiol - DMSO)
*
N.S.
N.S.
n = 145 152 148
c
Gene body
Promoter
JA-IR
Random
Stably expr.
Frequency
Number of unique genes
Alignment length (nt)
ATREP2 ATREP7 TNAT1A
d
ST p = 0.000
G p = 0.024
STxG p = 0.001
Larval weight (mg)
Col-0
ago1-45
ago1-46
e
1. Naïve state
ATREP2
RdDM
JA defence gene
JA induction
2. IR elicitation
ROS1
Basal induction
MYC
3. IR maintenance
PTGS
AGO1
Primed / weakly upregulated
JA challenge
4. IR expression
Augmented induction

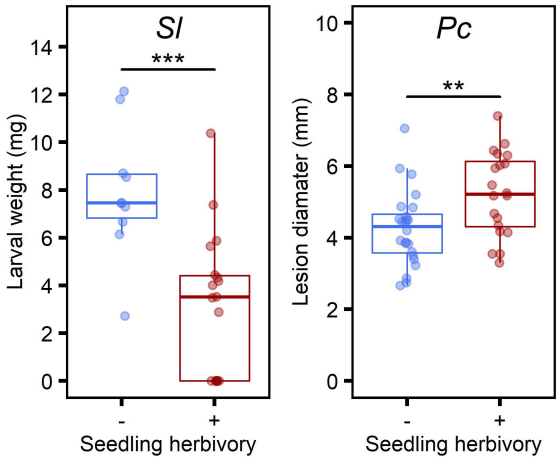
Sl
***
Larval weight (mg)
0
2
4
6
8
10
12
14
-
+
Seedling herbivory
Pc
**
Lesion diamater (mm)
0
2
4
6
8
10
-
+
Seedling herbivory

a

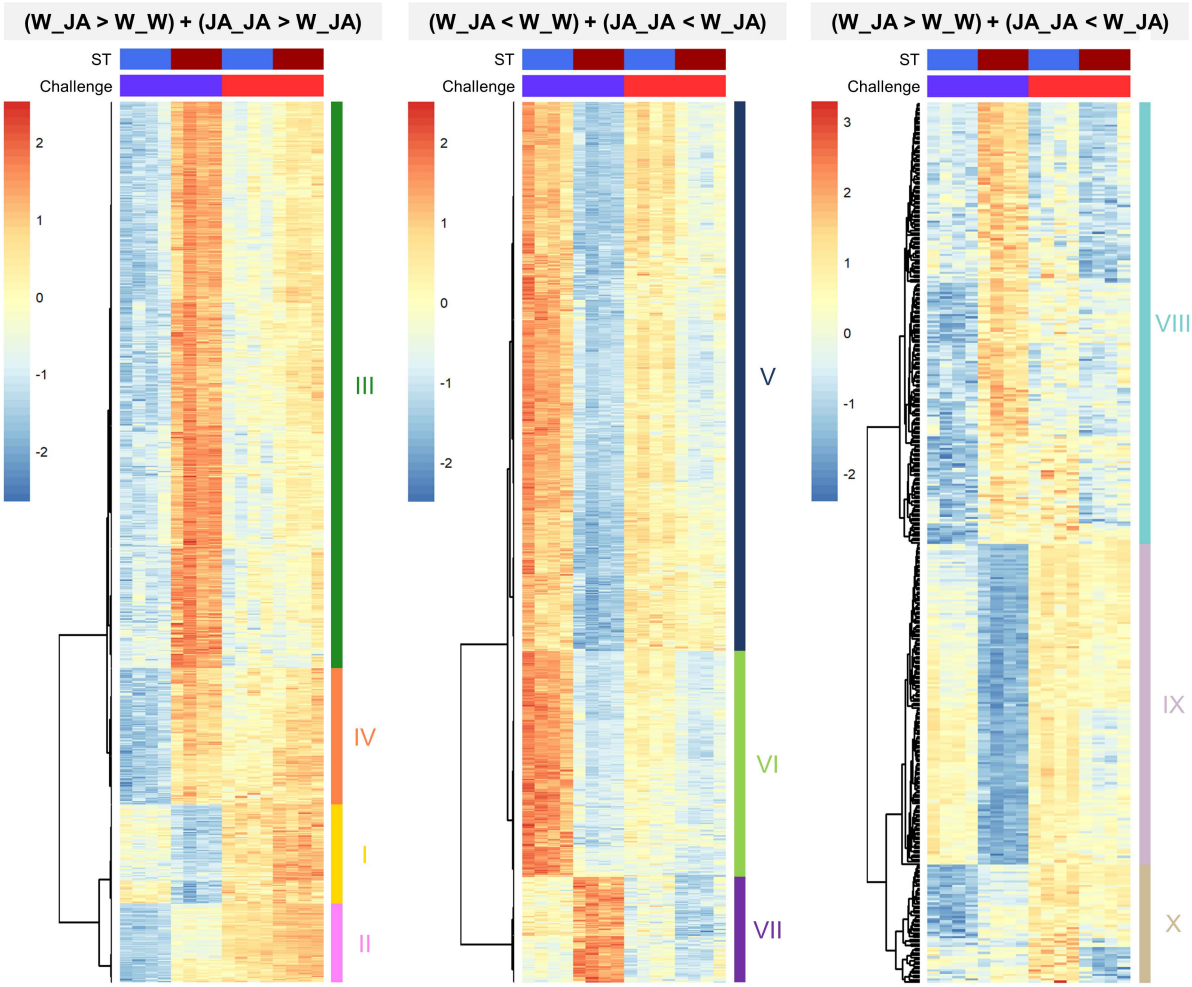

b

Cluster	GO term	GO name	Fold enrichment
II	GO:0009694	jasmonic acid metabolic process	9.60
II	GO:0019760	glucosinolate metabolic process	8.97
II	GO:0009753	response to jasmonic acid	7.68
II	GO:0009611	response to wounding	5.50
IV	GO:0019761	glucosinolate biosynthetic process	7.99

Cluster	GO term	GO name	Fold enrichment
V	GO:0052542	defense response by callose deposition	4.89
V	GO:0009863	salicylic acid mediated signaling pathway	4.27
V	GO:0009627	systemic acquired resistance	3.96
VI	GO:0050832	defense response to fungus	5.11
VI	GO:0009626	plant-type hypersensitive response	4.98
VI	GO:0042742	defense response to bacterium	3.04

Cluster	GO term	GO name	Fold enrichment
IX	GO:0009693	ethylene biosynthetic process	5.58
IX	GO:0009873	ethylene-activated signaling pathway	5.33
IX	GO:0009620	response to fungus	4.58
IX	GO:0009867	jasmonic acid mediated signaling pathway	3.98
IX	GO:0010200	response to chitin	3.63
IX	GO:0009863	salicylic acid mediated signaling pathway	3.28

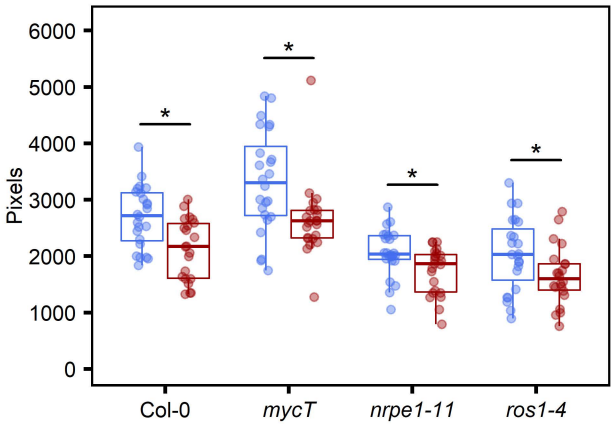
6000
5000
4000
3000
2000
1000
0
Pixels
*
*
*
*
Col-0
mycT
nrpe1-11
ros1-4

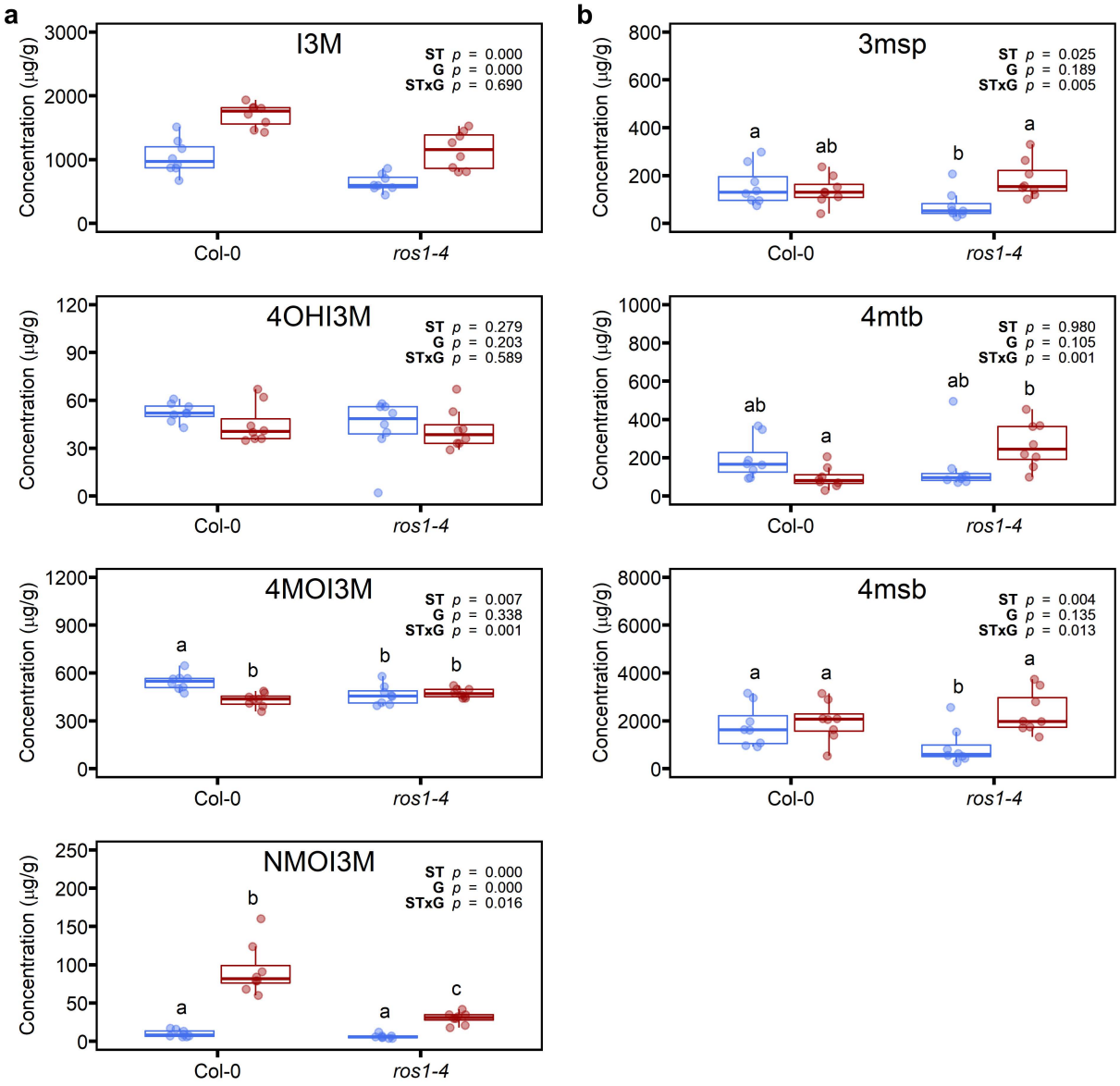
a
b
I3M
ST p = 0.000
G p = 0.000
STxG p = 0.690
3msp
ST p = 0.025
G p = 0.189
STxG p = 0.005
4OHI3M
ST p = 0.279
G p = 0.203
STxG p = 0.589
4mtb
ST p = 0.980
G p = 0.105
STxG p = 0.001
4MOI3M
ST p = 0.007
G p = 0.338
STxG p = 0.001
4msb
ST p = 0.004
G p = 0.135
STxG p = 0.013
NMOI3M
ST p = 0.000
G p = 0.000
STxG p = 0.016
Concentration (µg/g)
Col-0
ros1-4

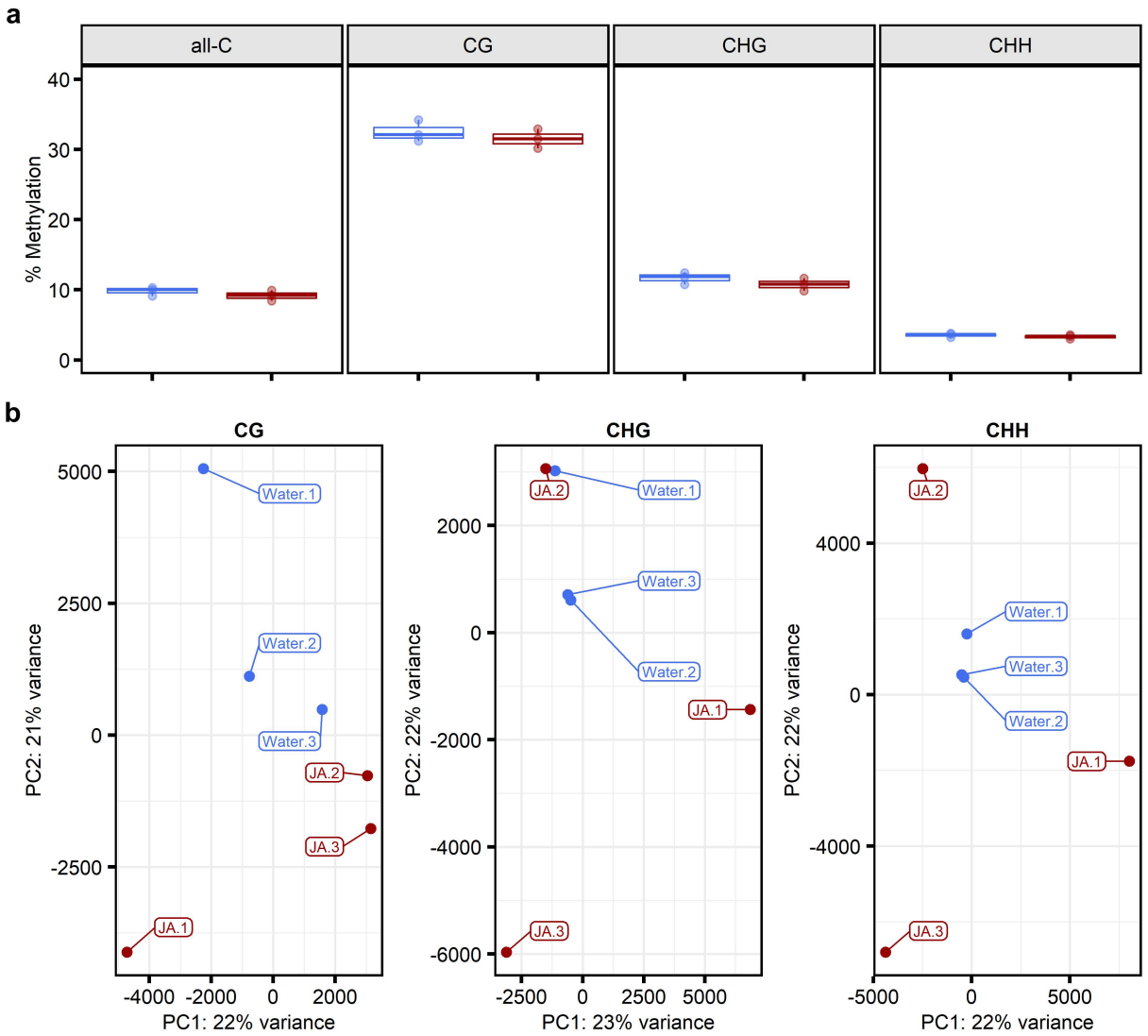
a
all-C
CG
CHG
CHH
% Methylation
40
30
20
10
0
b
CG
CHG
CHH
PC2: 21% variance
PC2: 22% variance
PC2: 22% variance
PC1: 22% variance
PC1: 23% variance
PC1: 22% variance
Water.1
Water.2
Water.3
JA.1
JA.2
JA.3
5000
2500
0
-2500
2000
-2000
-4000
-6000
4000
-5000

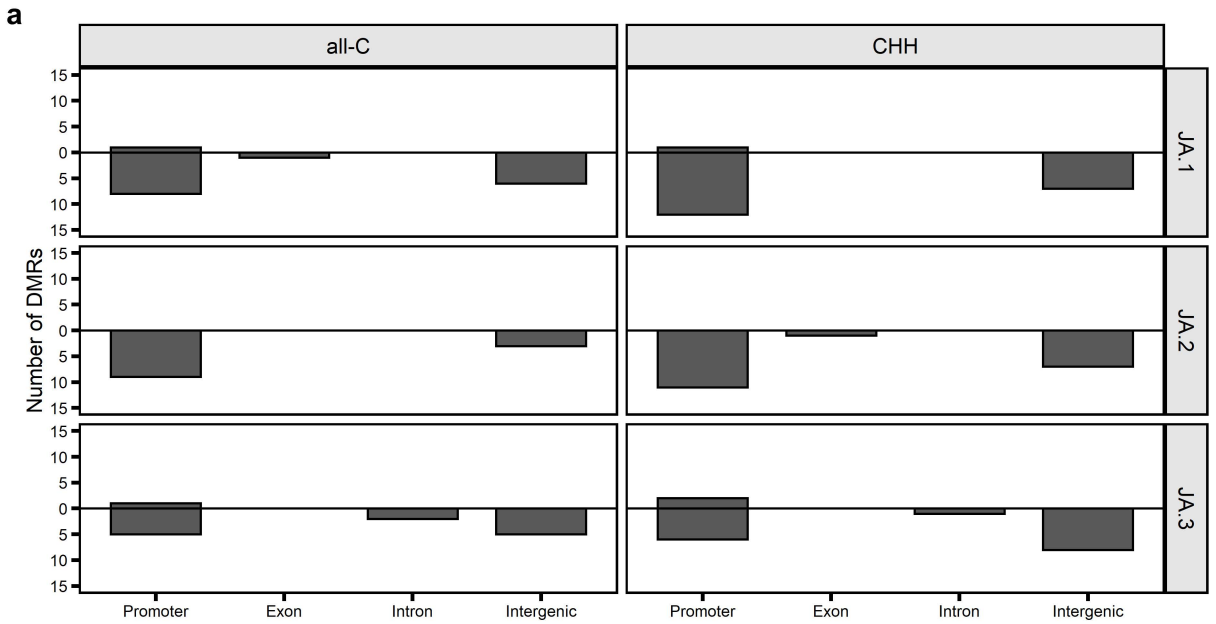
a
all-C
CHH
JA.1
JA.2
JA.3
Number of DMRs
15
10
5
0
5
10
15
Promoter
Exon
Intron
Intergenic

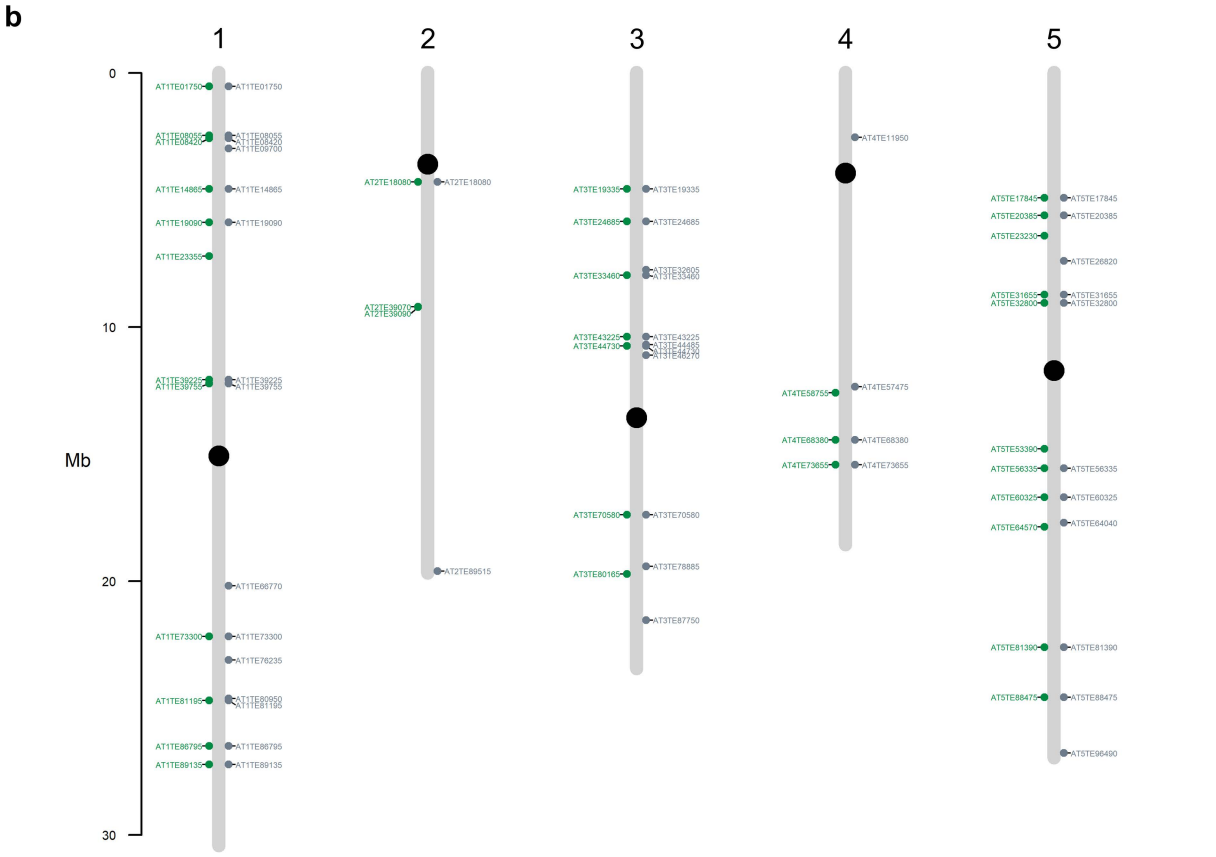
b
1
2
3
4
5
Mb
0
10
20
30
AT1TE01750
AT1TE08055
AT1TE08420
AT1TE09700
AT1TE14865
AT1TE19090
AT1TE23350
AT1TE39225
AT1TE39760
AT1TE68770
AT1TE73300
AT1TE76235
AT1TE80950
AT1TE81195
AT1TE86795
AT1TE89135
AT2TE18080
AT2TE39070
AT2TE89515
AT3TE19335
AT3TE24685
AT3TE33605
AT3TE33460
AT3TE43225
AT3TE44485
AT3TE44730
AT3TE46270
AT3TE70580
AT3TE78885
AT3TE80165
AT3TE87750
AT4TE11950
AT4TE57475
AT4TE58755
AT4TE68380
AT4TE73655
AT5TE17845
AT5TE20385
AT5TE23230
AT5TE26820
AT5TE31655
AT5TE32800
AT5TE53390
AT5TE56335
AT5TE60325
AT5TE64040
AT5TE64570
AT5TE81390
AT5TE88475
AT5TE96490

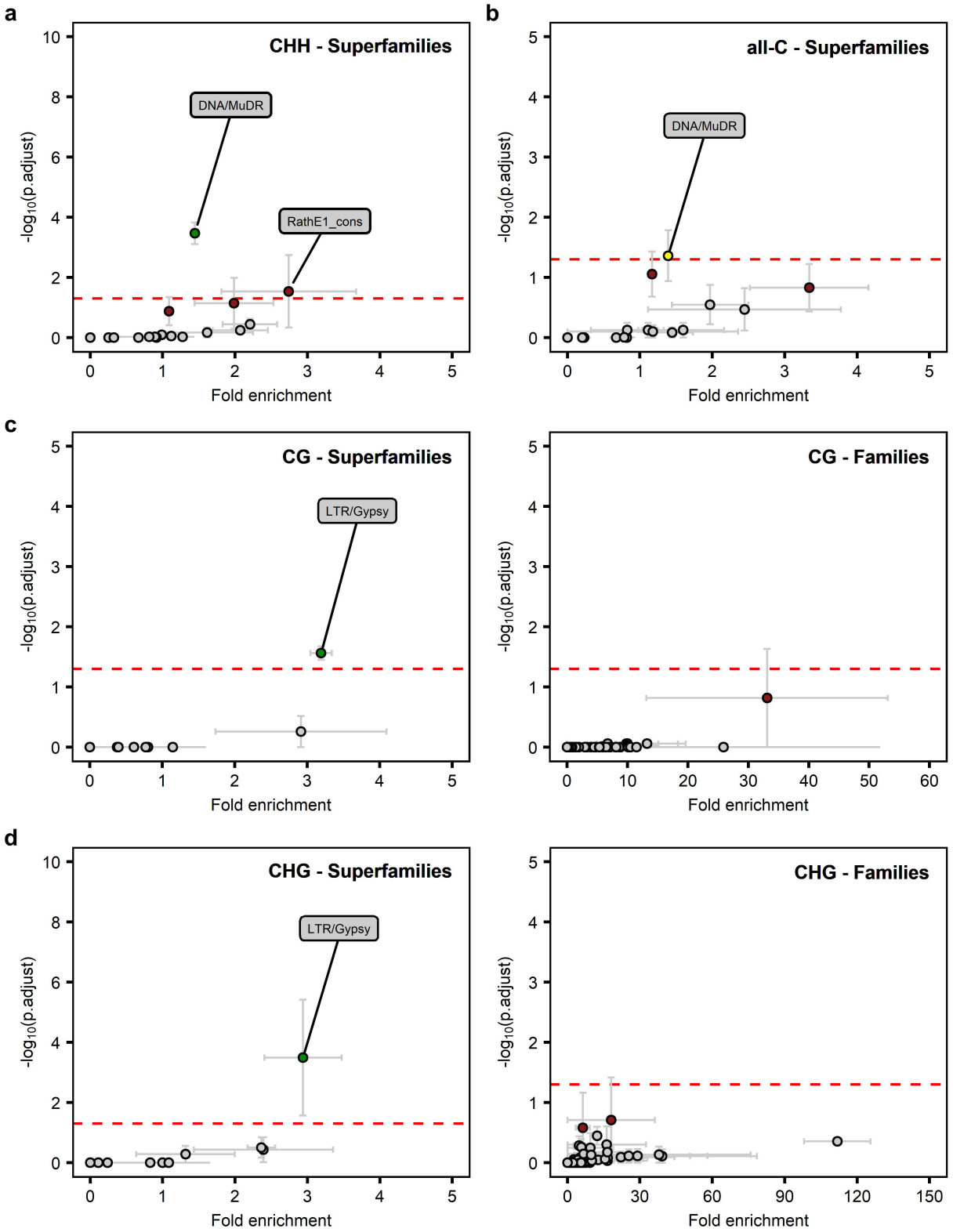
a
CHH - Superfamilies
DNA/MuDR
RathE1_cons
-log10(p.adjust)
Fold enrichment
b
all-C - Superfamilies
DNA/MuDR
-log10(p.adjust)
Fold enrichment
c
CG - Superfamilies
LTR/Gypsy
-log10(p.adjust)
Fold enrichment
CG - Families
-log10(p.adjust)
Fold enrichment
d
CHG - Superfamilies
LTR/Gypsy
-log10(p.adjust)
Fold enrichment
CHG - Families
-log10(p.adjust)
Fold enrichment

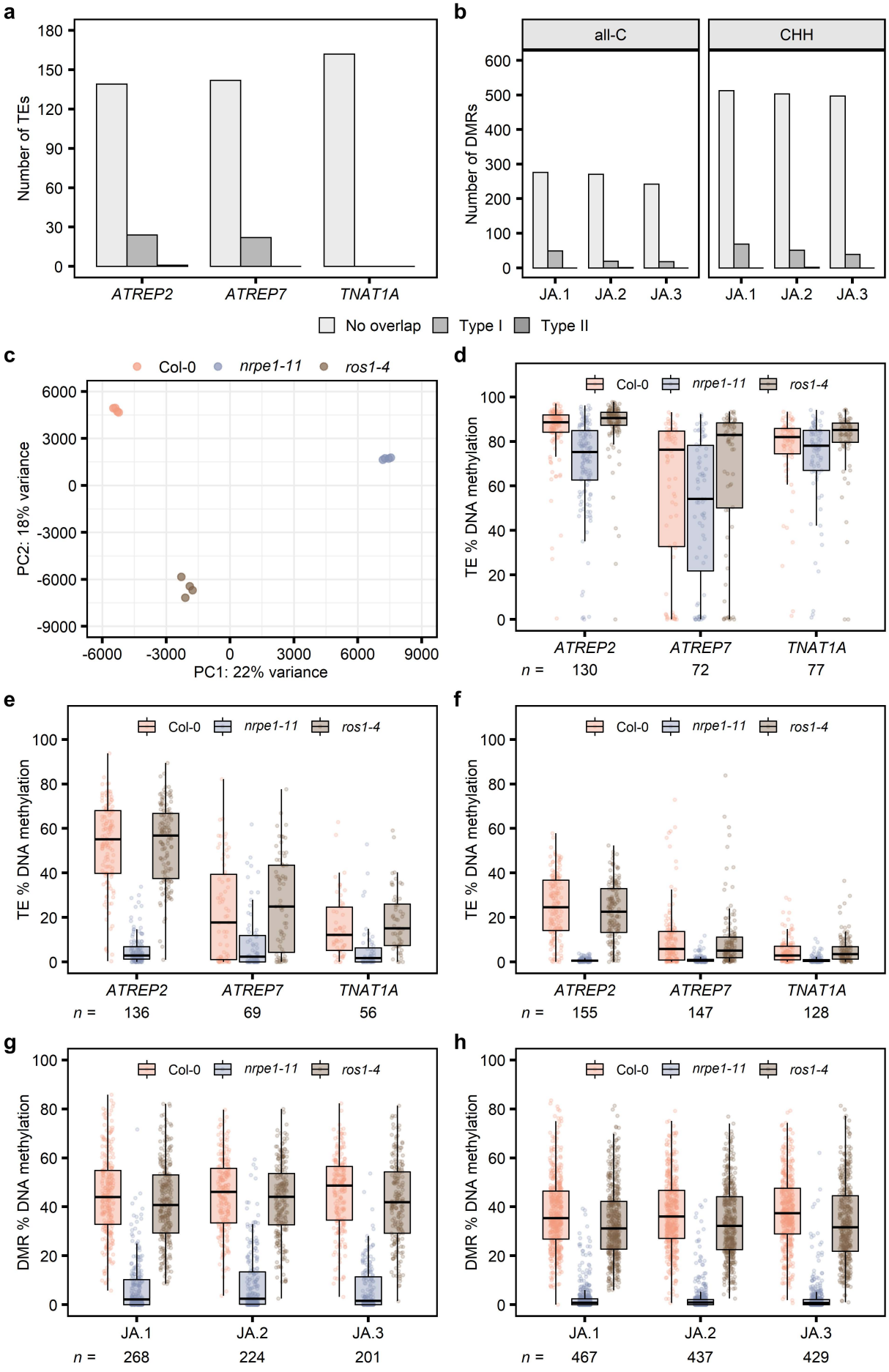
a
Number of TEs
180
150
120
90
60
30
0
ATREP2
ATREP7
TNAT1A
b
all-C
CHH
Number of DMRs
600
500
400
300
200
100
0
JA.1
JA.2
JA.3
No overlap
Type I
Type II
c
Col-0
nrpe1-11
ros1-4
PC2: 18% variance
PC1: 22% variance
6000
3000
0
-3000
-6000
-9000
d
TE % DNA methylation
n = 130 72 77
e
n = 136 69 56
f
n = 155 147 128
g
DMR % DNA methylation
n = 268 224 201
h
n = 467 437 429

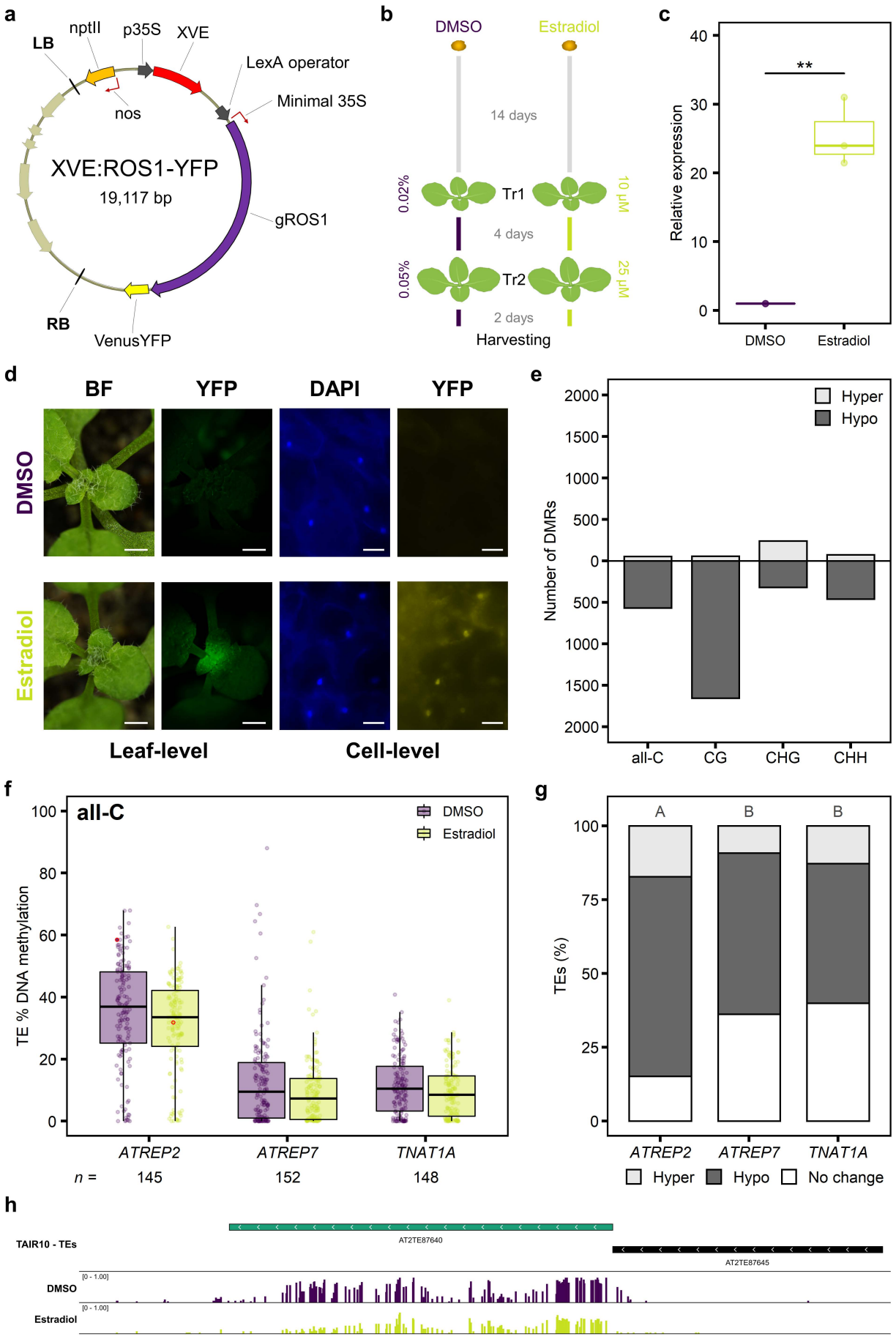
a
LB
nptII
p35S
XVE
LexA operator
Minimal 35S
nos
XVE:ROS1-YFP
19,117 bp
gROS1
RB
VenusYFP
b
DMSO
Estradiol
14 days
0.02%
Tr1
10 µM
4 days
0.05%
Tr2
25 µM
2 days
Harvesting
c
Relative expression
**
DMSO
Estradiol
d
BF
YFP
DAPI
YFP
DMSO
Estradiol
Leaf-level
Cell-level
e
Hyper
Hypo
Number of DMRs
all-C
CG
CHG
CHH
f
all-C
DMSO
Estradiol
TE % DNA methylation
ATREP2
ATREP7
TNAT1A
n = 145 152 148
g
A
B
B
TEs (%)
ATREP2
ATREP7
TNAT1A
Hyper
Hypo
No change
h
TAIR10 - TEs
AT2TE87640
AT2TE87645
DMSO
Estradiol

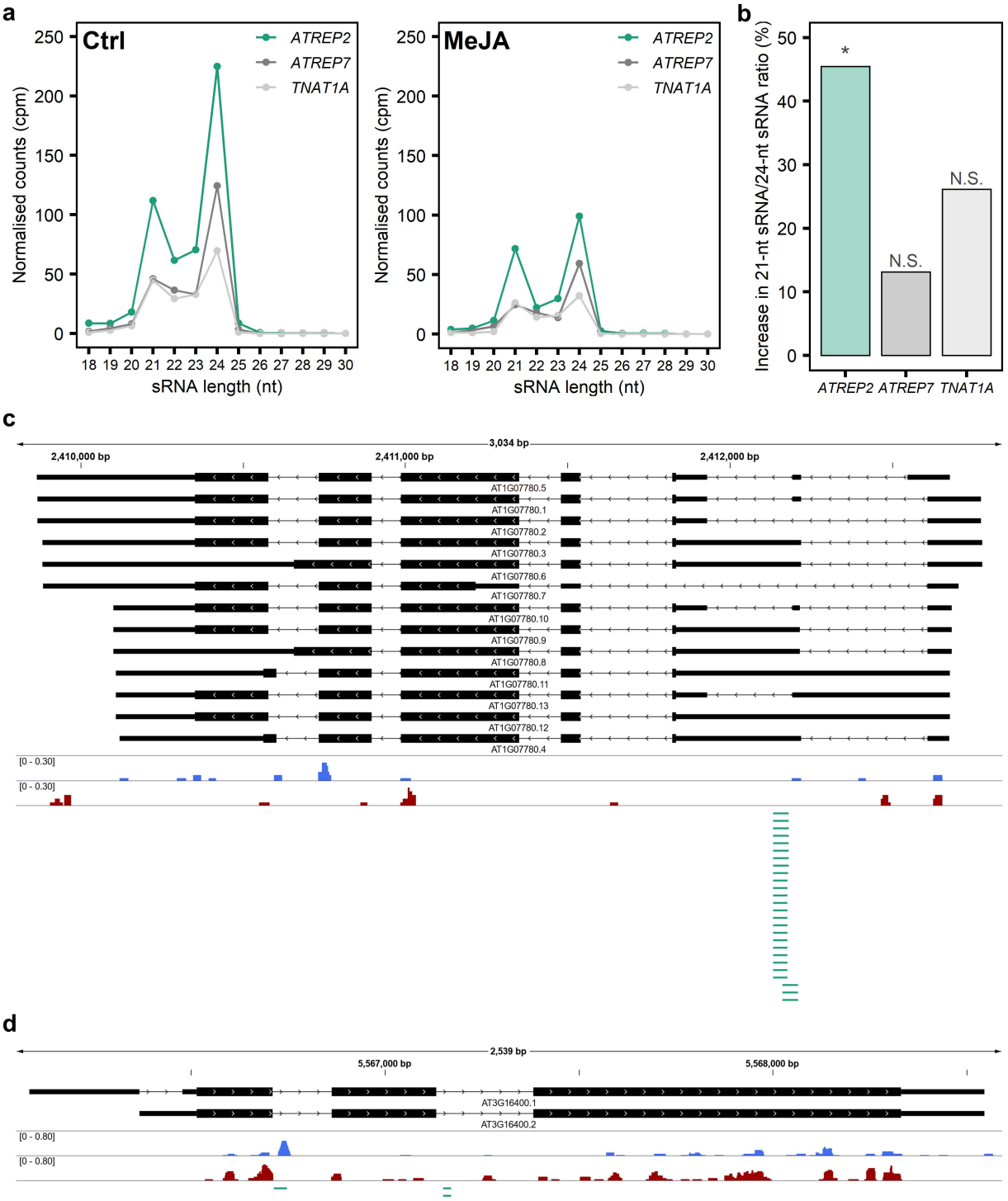
a
Ctrl
MeJA
ATREP2
ATREP7
TNAT1A
Normalised counts (cpm)
sRNA length (nt)
b
Increase in 21-nt sRNA/24-nt sRNA ratio (%)
*
N.S.
N.S.
ATREP2 ATREP7 TNAT1A
c
3,034 bp
2,410,000 bp
2,411,000 bp
2,412,000 bp
AT1G07780.5
AT1G07780.1
AT1G07780.2
AT1G07780.3
AT1G07780.6
AT1G07780.7
AT1G07780.10
AT1G07780.9
AT1G07780.8
AT1G07780.11
AT1G07780.13
AT1G07780.12
AT1G07780.4
[0 - 0.30]
[0 - 0.30]
d
2,539 bp
5,567,000 bp
5,568,000 bp
AT3G16400.1
AT3G16400.2
[0 - 0.80]
[0 - 0.80]

SUPPLEMENTARY METHODS

Plant materials and growth conditions.

The *ros1-4* (SALK_135293), *ago1-45* (NASC ID = N67861) and *ago1-46* (NASC ID = N67862) mutants were obtained from the Nottingham Arabidopsis Stock Centre (NASC) and the *nrpe1-11* (SALK_029919) mutant was kindly provided by Professor Pablo Vera (Instituto de Biología Molecular y Celular de Plantas, Spanish National Research Council, Spain). Seeds of *ros1-4* and *nrpe1-11* came from stocks that had previously been confirmed to carry the correct T-DNA insertions and display transcriptional knock-down of *ROS1* and *NRPE1* genes, respectively[1]. *ago1-45* and *ago1-46* seed stocks were confirmed to be the correct genotype using previously described derived cleaved amplified polymorphic sequences (dCAPS) assays[2]. The *myc2 myc3 myc4* triple mutant (*mycT*)[3] was kindly provided by Professor Roberto Solano (Centro Nacional de Biotecnología, Consejo Superior de Investigaciones Científicas (CNB-CSIC), Spain). The *XVE:ROS1-YFP* line was created in this study and is described in detail below.

Cultivation of microbes and insect rearing.

Plectosphaerella cucumerina strain *BMM* (*Pc*) was continuously cultured on potato dextrose agar (PDA) in the dark and at 15-25 °C. Four weeks prior to spore collection, a plug of *Pc* PDA was transferred to a new plate. *Pseudomonas syringae* pv. *tomato* DC3000 *luxCDABE* (*Pst*) was stored in the form of glycerol stocks at -80 °C. Two days prior to inoculation, a glycerol stock was thawed on ice and then cultured at 28 °C on King's B (KB) agar plates supplemented with rifampicin (50 µg ml^{-1}) and kanamycin (50 µg ml^{-1}). *Spodoptera littoralis* larvae were reared in-house on a semi-artificial diet, which was formulated based on the diets in refs.[4–6]. A full diet ingredient list is provided in Supplementary Table 1. The diet was prepared by autoclaving the agar in half the volume of water (300 ml) and then mixing with the additional ingredients.

Chemicals plant treatments.

Stock solutions were prepared by diluting jasmonic acid (JA; Sigma Aldrich, J2500), 1-aminocyclopropanecarboxylic acid (ACC; Sigma Aldrich, A3903), salicylic acid (SA; Sigma Aldrich, S3007) and β-Estradiol (estradiol; Sigma-Aldrich, E8875) in absolute ethanol (JA and SA; Fisher Scientific, E/0650DF/17), dimethyl sulfoxide (estradiol; Sigma-Aldrich, D4540) or deionised H_2O (ACC). Estradiol stocks were stored at -20 ˚C and thawed and diluted in deionised H_2O prior to treatment of plants. Solutions for plant hormone treatments were prepared by diluting stocks with deionised H_2O and supplementing with 0.02% of the surfactant silwet L-77 (LEHLE SEEDS, VIS-30). Pre-treatment was performed with 1 mM JA. Challenge consisted of 0.5 mM SA, 0.1 mM JA or 0.1 mM JA + 0.1 mM ACC. The controls for both the pre-treatment ('control') and challenge ('mock') consisted of deionised H_2O supplemented with 0.02% silwet containing the same percentage ethanol as the corresponding hormone solution.

Hyperspectral quantification of plant size.

Five-week-old plants (22-24 per treatment-genotype combination) were imaged, using a PlantScreen HC 900 hyperspectral imaging system (Photon Systems Instruments), consisting of a push-broom scanner with a halogen lamp light source and complementary metal-oxide-semiconductor detector (spatial resolution = 5 $px.mm^{-1}$ and spectral resolution = 0.8 nm) mounted on a motorised carriage, which travelled directly over trays of plants at 15 $mm\ s^{-1}$. The camera lens was positioned 20 cm above the rosettes and a 0.09 s exposure time was used. Raw intensity values were acquired for 480 wavebands across a 350-900 nm spectral range. Plant size was approximated based on rosette surface area (RSA), which was quantified as the number of pixels in an image associated with one plant (unit of biological replication). Segmentation of plants from their background was achieved using a four-step pipeline. (i) A calibrated reflectance image (R) was produced, with reflectance values for all wavebands and pixels being generated using the following equation:

$$(1) \qquad R = \frac{I_{Raw} - I_{dark}}{I_{light} - I_{dark}}$$

The intensity values were taken from one raw hyperspectral image (I_{raw}) and two reference images of the same white Teflon standard, one of which was taken in the light (I_{light}) and one in complete darkness (I_{dark}). (ii) The wider area of the calibrated image containing the plant of interest was defined. (iii) All pixels within the defined area with a plant index (equation 2) > 0.53 were selected.

$$(2) \qquad Plant\ index = 1.2\big(2.5(R_{740} - R_{672}) - 1.3(R_{740} - R_{556})\big)$$

(iv) Approximately one layer of pixels was removed from the edge of each selection of plant-associated pixels ('plant mask'). Computational analyses of the hyperspectral photos were performed with PlantScreen Data Analyser software v3.1.4.13 (Photon Systems Instruments) and R v3.6.1.

Construction of the XVE:ROS1-YFP binary plasmid and plant transformations.

DNA was extracted from Col-0 seedlings[7] and used for PCR to amplify genomic *ROS1* DNA (*gROS1*), using Phusion DNA polymerase (New England Biolabs, M0530S) and gene-specific primers (ROS1-F1: CACCGAAATGGAGAAACAGAGGAGAGAAG and ROS1-R1: GGCGAGGTTAGCTTGTTGTCCC). The amplified sequence included the CACC sequence at the 5'-end for directional cloning and excluded the stop codon at the 3'-end to enable the C-terminal fusion with *YFP*. The gDNA was cloned into a pENTR/D-TOPO plasmid and selected in TOP10 cells (Thermo Fisher Scientific, K240020). This *gROS1*-containing entry plasmid was used in a MultiSite Gateway recombination reaction with entry plasmids p1R4-p35S:XVE (containing the XVE gene; kindly provided by Ari Pekka Mähönen of the University of Helsinki, Finland)[8,9], and p2R3a-VenusYFP-3AT (containing the VenusYFP gene; Addgene, plasmid #71269)[8] and the empty binary destination plasmid pCAM-kan0R4R3 (Addgene, plasmid #71275)[8], according to manufacturer's recommendations (MultiSite Gateway Three-Fragment Vector Construction Kit; Thermo Fisher Scientific, 12537-023). The resulting 19,117 bp binary plasmid (XVE:ROS1-YFP; Extended Data Fig.

9a) was transformed into the *Agrobacterium* strain GV3101 by electroporation and selected on lysogeny broth 1.5% agar plates containing 50 mg/L rifampicin, 50 mg/L gentamycin and 50 mg/L kanamycin. All plasmids for sequencing and recombination reactions were extracted using the GeneJET Plasmid Miniprep Kit (Thermo Fisher Scientific, K0503). The *gROS1* sequence in the entry plasmid and the T-DNA sequence of the XVE:ROS1-YFP binary plasmid were validated by Sanger sequencing. Transformed GV3101 cells were used for floral-dip transformation of Arabidopsis (Col-0), after which T1 generation transgenic plants were selected for kanamycin resistance on 1/2-strength Murashige and Skoog agar plates containing 50 mg/L kanamycin[10]. In the T2 generation, a line displaying Mendelian 3:1 segregation of kanamycin resistance was identified, with homozygous individuals being carried through to the T3 generation. Homozygosity was verified in the T3 generation using kanamycin resistance and YFP fluorescence in response to estradiol treatment. The presence of a single insertion was confirmed using the Nanopore sequencing data described below.

Fluorescence microscopy to validate *in planta* accumulation of ROS1-YFP by estradiol.

Macroscopic photos of leaves were acquired with a Leica M165 FC fluorescent stereo microscope (Objective: 1x/0.06; ET-GFP filter set: 470/40 nm excitation, 495 nm dichroic and 525/50 nm emission), CoolLED *p*E-300 white illumination system and the Leica LAS X software v3.7.4.23463. The brightness of all macroscopic photos was increased by 40%.

Localization of ROS1-YFP to the nucleus was assessed by epifluorescence microscopy. Plants were incubated in DAPI solution (2 µg/ml), with vacuum infiltration used to aid the uptake of DAPI solution into the leaves. Plants were mounted on slides and imaged using a Leica DM6 B upright microscope (Objective: HC PL FLUOTAR 40x/0.80 DRY; GFP ET filter set: 470/40 nm excitation, 495 nm dichroic and 525/50 nm emission; DAPI ET filter set: 350/50 nm excitation, 400 nm dichroic and 460/50 nm emission), CoolLED *p*E-2 illumination system and the Leica LAS X software v3.7.4.23463. Using the LAS X software, DAPI and

YFP images were pseudo-coloured blue and yellow, respectively. Both the brightness and contrast of all YFP images were increased by 40%. For the DAPI images, brightness and contrast were increased by 30% and 70%, respectively.

Liquid chromatography coupled to mass spectrometry analysis of glucosinolates.

Extraction and quantification of glucosinolates was performed as described previously[11]. Briefly, 5 mg of dried tissue was ground to a fine powder. Glucosinolates were extracted by addition of 1 ml of 70% (v/v) methanol/water solution to the powder, vortexed, heated (5 min), shaken (15 min), centrifuged (5 min at 15000g), and the supernatant was transferred into new tubes. The supernatant was diluted in 100% Milli-Q water, filtered through a 0.22 µm KX syringe filter (PTFE 13 mm diameter; Mikrolab), and injected into the LC-MS/MS system.

Samples were analysed in multiple reaction mode (MRM) by an Agilent 1260 Infinity HPLC system (Santa Clara) connected to an AB Sciex 4500 triple-quadrupole trap (QqQ) mass spectrometer (QTRAP/MS; AB Sciex), equipped with electrospray ionization (ESI) source in negative ion mode. HPLC separation of samples occurred at 40 ˚C on a reversed-phase Synergi Fusion-RP C18, 80A column (250 mm × 2 mm i.d., 4 µm; Phenomenex) equipped with a Security Guard Cartridge (Phenomenex, KJ0-4282). A binary solvent mixture was used consisting of water (solvent A) and methanol (solvent B). Both solvents contained 20 mM acetic acid. The flow rate was 0.3 ml/min, and the injection volume 20 µl. The binary gradient was set up as follows: 0-3 min, column equilibration (95% A), 3-10 min, ramping to (80% A), 10-17 min, ramping to (55% A), 17-35 min, ramping to (0% A), 35-38 min, isocratic hold (0% A), 38-38.5 min, ramping back to (95% A), and 38.5-45 min, column re-equilibrating (95% A). For each compound, two MRM-transitions, which showed the best signal-to-noise ratios, were monitored. All data were collected using ABSciex Analyst software v1.6.2. Quantitation was performed using ABSciex MultiQuant software v3.0.2. Samples were run in a randomized order.

RNA extractions.

Two-week-old WT plants were treated with either water (control) or JA. A subset of plants were challenged 3 weeks later with a water (mock) or chemical solution (JA, SA, or JA + ACC), as detailed in the Methods. Leaf material was harvested both before and at 4 hrs, 24 hrs, 1 week and 3 weeks after seedling treatment (Fig. 1b) or at 4, 8 and 24 hrs after challenge treatment (Fig. 1e). For the seedling treatment only experiment (Fig. 1b), 2-6 similarly aged plants from the same tray (4 hrs, 24 hrs and 1 week) or 3-5 leaves of a comparable physiological age from a single plant (3 weeks), were pooled and used as units of biological replication (*n*=2-3). For the seedling treatment + challenge experiments (Fig. 1e), 8 similarly aged leaves from 2 plants in the same tray were pooled and used as the units of biological replication (*n*=2-4). To quantify *ROS1* gene expression in *XVE:ROS1-YFP* plants, above-ground tissue was collected at 48 hrs after the second spray treatment (Extended Data Fig. 9b) and following 2 hrs in the dark. Approximately 100 seedlings were pooled for one unit of biological replication (*n*=3). Total RNA extractions were performed as described previously[1,12].

Reverse transcriptase-quantitative PCR (RT-qPCR).

Genomic DNA removal and cDNA synthesis were performed as described previously[1,12], using approximately 1 µg of total RNA. The sample mixes were prepared with the Rotor-Gene SYBR Green PCR Kit (Qiagen) and run in a Rotor-Gene Q (Qiagen) real-time PCR cycler. Reactions were run at the following cycling conditions: 1 cycle of 10 mins at 95 °C and 35-40 cycles of 10 seconds at 95 °C and 40 seconds at 60 °C. C_t values were based on 'take-off' values calculated by the Rotor-Gene Q v2.3.5 software. C_t values from reactions with primers against *MYC2*, *VSP2*, *PDF1.2*, *PR1* and *ROS1* (Supplementary Table 2) were calculated relative to a single calibrator sample, using real-time PCR efficiency values (E+1) of each primer pair. For each sample, the resulting values were normalised to the average values of 2 or 3 of the reference genes, *GAPC2* (*AT1G13440*), *UBC21* (*AT5G25760*) and *MON1* (*AT2G28390*), and normalised against the mean relative expression values of

replicates harvested prior to seedling treatment (Fig. 1b), at 4 hrs after mock challenge of water seedling treated plants (Fig. 1e) or 48 hrs after DMSO treatment of *XVE:ROS1-YFP* plants (Extended Data Fig. 9c).

mRNA-sequencing analysis: library preparation and sequencing.

The mRNA-sequencing (mRNA-seq) analysis was based on the same total RNA extracts used for RT-qPCR analysis of *VSP2* expression at 4 hrs after water/JA challenge (*n*=4; Fig. 1d). Quantity and quality of RNA was assessed using a Nanodrop and 2100 Bioanalyzer (Agilent Technologies). All RNA extracts used for sequencing yielded RNA integrity numbers (RIN) of at least 6.4. Isolation of mRNA via oligo dT-based selection for poly(A) tails, library preparation and sequencing was performed by BGI Genomics. Sequencing was performed with the BGISEQ-500 platform functioning in its single end mode. Across all 16 samples 598 million 50 bp single-end clean reads were generated, with an average of 37.4 million clean reads per sample (Supplementary Data 19). On average 98.7% of nucleotides per sample had a Phred quality score of > 20 (Supplementary Data 19).

mRNA-sequencing analysis: read alignment and counting.

Read quality was assessed using FASTQC v0.11.5 (http://www.bioinformatics.babraham.ac.uk/projects/fastqc/) and MultiQC v1.7[13]. The first 15 bases of reads were removed using the read trimming tool Trimmomatic v0.38 (options: 'SE', 'HEADCROP:15')[14]. Reads were aligned to the Arabidopsis genome (Ensembl Plants vTAIR10.40), using STAR v2.6.1b with default parameters[15]. All samples had read alignment efficiencies between 89.3-90.8% (average 90.3%; Supplementary Data 19). Numbers of reads mapping to each annotated gene were counted using HTSeq v0.9.1 (option: '--stranded=no')[16].

mRNA-sequencing analysis: statistical analysis of global transcriptome patterns and differentially expressed genes.

Read count tables were loaded into R v3.6.1 and genes with a total read count of < 100 across all samples were removed. Read counts were normalised for library size and transformed with a variance stabilising transformation (VST)[17]. Principal component analysis (PCA) of the 16 samples was performed using the 'plotPCA' function from DESeq2 v1.24.0[18] and displayed with ggplot2 v3.2.1. The outcome of hierarchical cluster analysis (HCA) of the 16 samples was displayed using pheatmap v1.0.12, with the complete linkage clustering method and Euclidean distances.

To identify differentially expressed genes (DEGs) associated with long-term JA-induced changes in resistance against JA-eliciting attackers, we used DESeq2[18] to select for expression profiles with a statistically significant interaction between JA seedling treatment and JA challenge treatment. A total of 2,409 DEGs were selected with an FDR-adjusted *p*-value (*p.adj*) < 0.01 (Supplementary Fig. 1). These represented genes that responded differently to JA challenge as a result of JA seedling treatment. The expression profiles were projected in a clustered heatmap by the 'aheatmap' function of NMF v0.21.0, using Ward's method and Pearson correlation distances. VST-transformed count data were projected in the heatmap as per gene z-scores.

To identify DEGs associated with the long-term JA-IR against *Sl*, genes were selected based on their expression profile across the four treatment combinations (W_W, JA_W, W_JA, JA_JA; first letters indicate seedling treatment and second letters challenge treatment). Selected genes had to (i) be upregulated in response to JA challenge in plants from water-treated seedlings (W_JA > W_W) and (ii) exhibit augmented expression after JA challenge in plants from JA-treated seedlings compared to plants from water-treated seedlings (JA_JA > W_JA). A clustered heatmap displaying the resulting 832 genes was created using Ward's clustering method and Spearman distances (Extended Data Fig. 2a). Based on expression profiles and enrichment of gene ontology (GO) terms related to anti-herbivore defences (see

below), clusters II and IV with a total of 203 genes were selected for further analysis. This final set of IR-related genes were projected in a clustered heatmap using Ward's clustering method and Pearson distances (Fig. 2c).

DEGs were selected as associated with long-term JA-IS against *Pst* if they (i) were downregulated in response to JA challenge in plants from water-treated seedlings (W_JA < W_W) and (ii) exhibited reduced expression after JA challenge in plants from JA-treated seedlings compared to plants from water-treated seedlings (JA_JA < W_JA). The resulting 904 genes were displayed in a clustered heatmap using Ward's clustering method and Pearson distances (Extended Data Fig. 2a). Based on expression profiles and enrichment of GO terms relating to anti-pathogen defences (see below), clusters V and VI with a total of 796 genes were selected and displayed in a clustered heatmap created as before (Fig. 2c).

DEGs were selected as being associated with long-term JA-IS against *Pc* if they (i) were upregulated in response to JA challenge in plants from water-treated seedlings (W_JA > W_W) and (ii) showed reduced expression after JA challenge in plants from JA-treated seedlings compared to plants from water-treated seedlings (JA_JA < W_JA). The resulting 395 genes were displayed in a clustered heatmap using the average clustering method and Spearman distances (Extended Data Fig. 2a). Based on expression profile and enrichment of GO terms relating to anti-pathogen defences (see below), cluster IX with a total of 144 genes was selected and displayed in a clustered heatmap created as before (Fig. 2c).

mRNA-sequencing analysis: statistical enrichment analyses of gene ontology terms and TF DNA-binding motifs.

GO term enrichment analysis was performed with R packages clusterProfiler v3.12.0 and org.At.tair.db v3.8.2. For analysis of single and multiple gene clusters, the clusterProfiler functions 'compareCluster' and 'enrichGO', respectively, were used with parameters: 'universe = all genes with ≥ 100 counts across all 16 samples', 'fun = "enrichGO"' ('compareCluster' only), 'OrgDb = 'org.At.tair.db'', 'keyType = "TAIR"', 'ont = 'BP'',

'minGSSize = 10' and 'maxGSSize = 500'. Biological process GO terms with a *p.adj* < 0.05 were classed as enriched. Fold enrichment plots of selected enriched defence-related GO terms were created using the R package ggplot2 v3.2.1.

For the TF DNA-binding motif enrichment analysis, promoter sequences (TSS to 1 kb upstream) for all genes analysed by DESeq2 (≥ 100 reads across all samples), were downloaded from TAIR v10. These promoter sequences, together with the 803 Arabidopsis TF DNA-binding motifs found in the MotifDb v1.26.0 R package and the functions 'makePriors', 'PFMtoPWM' and 'makeBackground' from the PWMEnrich v4.20.0 R package, were used to create background distributions of TF DNA-binding motifs. To determine which of the 803 MotifDb Arabidopsis motifs were significantly overrepresented ($p < 0.01$) in the 203 IR-related genes promoters relative to the background, the PWMEnrich functions 'motifEnrichment' (all parameters default apart from 'group.only = F') and 'groupReport' (all options default) were used. Sequence logos were produced using the PWMEnrich 'plot' function.

Whole-genome bisulfite sequencing (WGBS) analysis: read alignment.

Reads were assessed for quality using FASTQC v0.11.5 and MultiQC v1.7[13] and trimmed using Trimmomatic v0.38 (Options: W vs JA experiment 'HEADCROP:10'; Methylation mutant experiment 'SLIDINGWINDOW:4:25', 'HEADCROP:6', MINLEN:36')[14]. Reads were aligned to the Arabidopsis genome (TAIR10) using bismark v0.21.0[19], run with the default parameter settings which includes the use of Bowtie2 v2.3.4.1[20] for read mapping. Alignment efficiency was between 52-66% (Supplementary Data 20 and 21). To remove duplicate reads, BAM alignment files were rearranged using SAMtools v1.7 (options: 'sort', '-n')[21] and then passed to the Bismark tool 'deduplicate_bismark' (option: '--paired'). Between 4-47% of aligned paired-end reads were removed from each sample in the deduplication procedure. After alignment and deduplication, between 32-54% of all sequenced paired-end reads were retained per sample (Supplementary Data 20 and 21).

WGBS analysis: methylation calling and determining weighted methylation levels.

Methylated and total (methylated + unmethylated) read counts per cytosine (C) position were generated using the Bismark v0.21.0 tool 'bismark_methylation_extractor' (options: '--paired-end', '--no_overlap', '--ignore_3prime_r2 90', '--comprehensive', '--bedGraph', '--CX', '--cytosine_report'). Per sample bisulfite treatment non-conversion rates were estimated from the unmethylated plastid genome and ranged between 0.37-0.54% (Supplementary Data 20 and 21; non-conversion rate < 2% is considered acceptable[22]). Counts for all C positions in the nuclear genome were used for downstream analysis of genome-wide methylation at all sequence contexts (all-C), as well as for CG, CHG and CHH contexts separately (H indicates any base other than G). Estimates of genome-wide methylation levels were calculated using the weighted methylation level equation in ref.[23].

WGBS analysis: global analysis of positional cytosine methylation.

To detect global shifts in DNA methylation, for the 6 'W vs JA experiment' samples (Supplementary Data 20) HCAs and PCAs were conducted for each of the 4 sequence contexts (all-C, CG, CHG and CHH) and for the 'Methylation mutant experiment' a PCA was conducted for all-C. All analyses were performed with positional C-methylation data calculated using the site methylation level equation in ref.[23]. All C positions with a coverage < 5 in one or more samples were removed. In addition, positions with a standard deviation of methylation lower than or equal to the median of the standard deviations of all cytosines across the whole genome were removed, thereby focusing the analyses on the most variable positions. PCAs were conducted with the R function 'prcomp' (options: 'center = TRUE', 'scale = FALSE'). HCA was performed with the R functions 'dist' and 'hclust' run with the options 'method = "euclidean"' and 'method = "average"', respectively. PCA and HCA plots were created with the R packages ggplot2 v3.2.1 and dendextend v1.13.4.

WGBS analysis: analysis of differentially methylated regions in JA-treated plants.

Since the global methylome analyses revealed increased variation in DNA methylation between replicate samples from plants of JA-treated seedlings, we adjusted our strategy for statistical selection of differentially methylated regions (DMRs) by selecting for DMRs that were statistically different between each individual sample from JA-treated plants and all three replicate samples from water-treated plants (1JA_vs_3W). This approach is not confounded by the increased variability between JA samples. To identify DMRs in each of the three all-C context 1JA_vs_3W comparisons, we used the DSS v2.26.0 R package functions 'DMLtest' (options: 'equal.disp = TRUE', 'smoothing = FALSE') followed by 'callDMR' (options: 'delta = 0.1', 'p.threshold = 0.05', 'minlen = 25', 'minCG = 5', 'dis.merge = 50', 'pct.sig = 0.5')[24,25]. Since DSS accounts for coverage depth information, we included all C positions. Context-specific DMRs were identified by running the same DSS analysis pipeline with C positions at CG, CHG or CHH contexts only.

To map DMRs to genomic features, Arabidopsis genome and TE annotation files were downloaded from Ensembl vTAIR10.40 and TAIR v10, respectively. Analysis of DMRs overlapping with specific genomic features was conducted with the R packages GenomicRanges v1.36.1 and genomation v1.16.0. The precedence order for DMRs overlapping with genomic features was promotor > exon > intron > intergenic. Statistical enrichment of TE (super)families within DMRs was determined by hypergeometric tests, using all TEs annotated in TAIR v10 as the background (*p.adj* < 0.05). Plots of DMR frequencies and TE (super)family enrichments were created using the R packages ggplot2 v3.2.1 and ggrepel v0.8.1. A chromosome map displaying the distribution of DMR-overlapped *ATREP2* TEs was generated using the TAIR v10 gaps track downloaded from the UCSC genome browser, the centromere coordinates obtained from the TAIR v9 genome assembly and the R package chromPlot v1.12.0.

Consensus DMRs were defined as wider regions encompassing one DMR from each of the three 1JA_vs_3W comparisons, and were selected using the following pipeline: (i) identified

overlapping DMRs from a pair of 1JA_vs_3W comparisons, using the 'findOverlaps' function from the R package GenomicRanges, (ii) created merged DMRs using the highest and lowest coordinates from across the DMR pair, (iii) identified DMRs from the third 1JA_vs_3W comparison which overlapped merged DMRs, using the 'findOverlaps' function, (iv) created consensus DMRs using the highest and lowest coordinates from across the three DMRs, (v) repeated steps i to iv three times to cover each possible combination of 1JA_vs_3W comparisons, and (vi) removed consensus DMR duplicates. The consensus DMR identification pipeline was run twice for each of the 4 sequence contexts (all-C, CG, CHG and CHH). In the first run, pairs of DMRs were classed as overlapping if they were within 100 bp of one another and in the second run if they were within 500 bp of one another.

WGBS analysis: calculating methylation levels of JA-induced DMRs and TEs in methylation mutants.

For each genotype in the 'Methylation mutant experiment' (Col-0, *ros1-4*, *nrpe1-11*), read counts mapping to each cytosine position were pooled across 4 biological replicates. Methylation percentage for each position was calculated as: (number of methylated reads / total number of reads) * 100. The DMRs from 1JA_vs_3W comparisons in all-C and CHH contexts and TEs from the families *ATREP2*, *TNAT1A*, and *ATREP7* (TAIR v10) were intersected with genotype-specific methylation percentage files using bedtools intersect v2.30.0[26]. To finalise the lists of DMRs/TEs for use in cross-genotype comparisons of percentage methylation, the following sequential filtering steps were used on a context specific basis: (i) cytosine positions were removed if they had insufficient coverage (<5) in one or more of the three genotypes, (ii) DMRs/TEs were removed if they now had < 5 cytosine positions or if < 50% of their cytosine positions remained. Box plots displaying % methylation at DMRs/TEs present in all three genotypes were created with the R package ggplot2 v3.2.1.

WGBS analysis: identifying overlaps between type I / type II RdDM targets and TEs or JA-induced DMRs.

Lists of type I and type II RdDM loci in Col-0 were kindly provided by Tang and colleagues[27]. The R package GenomicRanges v1.36.1 was used to identify JA-induced DMRs (all-C and CHH) and TEs (*ATREP7*, *ATREP2*, *TNAT1A*) that overlap with RdDM-targeted loci. Frequency plots displaying DMRs/TEs overlapping with RdDM-targeted loci were created with the R package ggplot2 v3.2.1.

Oxford Nanopore Technologies (ONT) analysis of DNA methylation: library preparation and sequencing.

At 48 hrs after the second spray treatment with DMSO or estradiol (Extended Data Fig. 9b) and following 2 hrs in the dark, aerial tissue from ~100 *XVE:ROS1-YFP* seedlings (c. 500 mg fresh weight) was harvested, flash frozen and stored at -80 ˚C. DNA was extracted from frozen tissue using the NucleoBond® HMW DNA kit (Macherey Nagel, 740160.20) according to the manufacturer's instructions. DNA quality and quantity were assessed using a Nanodrop 8000 spectrophotometer and a Qubit 3.0 Fluorometer.

Library preparation was conducted using the Rapid Barcoding kit (ONT, SQK-RBK004). The prepared library was loaded into the FLO-MIN106 flow cell (FC) of a MinION sequencer (ONT). After 2 days, some FC pores (~37%) were recovered using the Flow Cell Wash Kit (ONT, EXP-WSH004), and a fresh library preparation was loaded. The FC was then run to exhaustion (~2 days).

Raw .fast5 files were basecalled and filtered using Guppy v6.0.1 ('guppy_basecaller --config dna_r9.4.1_450bps_hac.cfg'). This generated 382,253 reads with an average length of 8,913 bp for the DMSO replicate (3.7 Gb data; ~27x coverage; N50 = 17,042 bp), and 782,712 reads with an average length of 9,768 bp for the estradiol replicate (8.2 Gb data; ~60x coverage; N50 = 17,042). Summary statistics were obtained using NanoPlot v1.39.0.

ONT analysis of DNA methylation: methylation calling and downstream analysis.

Methylated cytosines were identified using DeepSignal-plant v0.1.4[28]. Base-called sequences were annotated onto raw .fast5 files ('tombo preprocess annotate_raw_with_fastqs') and resquiggled ('tombo resquiggle'; options: '--signal-length-range 0 1000000', '--sequence-length-range 0 100000'), using Tombo v1.5.1 and the Arabidopsis reference genome TAIR v10. Methylation predictions for all cytosines in the genome were called using DeepSignal-plant ('deepsignal_plant call_mods'), with the model 'model.dp2.CNN.arabnrice2-1_120m_R9.4plus_tem.bn13_sn16.both_bilstm.epoch6.ckpt'. The frequency of methylation at each CG, CHG, and CHH site was then called using DeepSignal-plant ('deepsignal_plant call_freq').

To identify DMRs between estradiol- and DMSO-treated *XVE:ROS1-YFP* plants, methylation frequency files were analysed using DSS v2.26.0, with functions 'DMLtest' (options: 'equal.disp = TRUE', 'smoothing = FALSE') and 'callDMR' (options: 'delta =0.1', 'p.threshold = 0.05', 'minlen = 25', 'minCG = 3', 'dis.merge = 50', 'pct.sig = 0.5')[24,25].

To compare methylation levels of *ATREP2*, *ATREP7* and *TNAT1A* TEs between estradiol- and DMSO-treated *XVE:ROS1-YFP* plants, methylation frequency files were intersected with the TAIR v10 TE annotation file using bedtools intersect v2.30.0[26], after which they were filtered as described for the WGBS methylome analysis. TEs were classed as being hypomethylated, hypermethylated or unchanged in the estradiol sample relative to the DMSO control based on a 1 percentage point change threshold. Pair-wise Chi-squared tests were used to identify TE families displaying statistically different distributions of the three classes (hypomethylated, hypermethylated and unchanged; $p.adj < 0.05$). DMR and TE % DNA methylation plots were created using the R package ggplot2 v3.2.1. Genome browser snapshots were created from IGV v2.8.6[29].

Analysis of sRNAs associated with nuclear AGO1.

Adaptors were trimmed from reads and low-quality reads were removed using Trim Galore v0.6.2 (options: '--quality 0', '--length 18', '--max_length 30', '--stringency 6', '--max_n 0'). Quality of the remaining reads was assessed using FASTQC and MultiQC[13]. Reads were mapped to the Arabidopsis genome (Ensembl Plants vTAIR10.40) using Bowtie v1.3.0 (options: '-v 0', '--all', '--best', '--sam', '--no-unal'), with all alignments with no mismatches being reported. To focus the analysis on siRNAs plausibly involved in the *trans*-regulation of JA-dependent defence genes by hypomethylated TEs, SAMtools v1.7[21], bedtools v2.30.0[26] and Picard v2.24.2 were used to remove reads mapping to known classes of RNAs (rRNAs, rRNAs, snRNAs, snoRNAs and miRNAs). Subsequently the same tools were used to calculate the number and size of sRNAs mapping to TEs of the *ATREP2*, *ATREP7* and *TNAT1A* families. Coordinates of known classes of RNAs and TEs annotated in the Arabidopsis genome were downloaded from TAIR v10. Chi-squared tests were used to identify TE families showing a statistically significant increase in the 21-nt sRNA to 24-nt sRNA ratio by MeJA ($p < 0.05$). The sRNA size against frequency distribution and 21-nt sRNA/24-nt sRNA ratio increase plots were created with the R package ggplot2 v3.2.1.

Analysis of sequence homology between *ATREP2* TEs and the 203 IR-related genes.

The 1000 bp promoters and genomic sequences of the 203 IR-related genes (Supplementary Data 4) were downloaded from TAIR v10 along with two control gene sets consisting of either 203 randomly selected genes or 203 stably expressed genes selected from Czechowski et al[30]. The three gene sets were converted into individual BLAST nucleotide databases using the BLAST+ v2.11.0[31] tool makeblastdb (options: '-parse_seqids' '-dbtype nucl'). Genomic sequences of all *ATREP2*, *ATREP7* and *TNAT1A* TEs were extracted from the Arabidopsis genome (Ensembl Plants vTAIR10.40), using bedtools v2.30.0[26]. Sequences of each TE family were individually queried against the three nucleotide databases using the BLAST+ tool blastn (options: '-word_size 7', '-evalue 0.05'). Results were filtered to retain alignments with a length ≥ 19 and ≤ 300. All alignments to

genes overlapping TEs from the family being queried were removed. Filtered alignments were displayed in histograms created using the R package ggplot2 v3.2.1 and together with AGO1-associated sRNAs in genome browser snapshots produced from IGV v2.8.6[29].

Statistical analysis of data from plant-interaction bioassays, hyperspectral imaging, glucosinolate profiling and RT-qPCR.

All statistical analyses were performed in R v3.6.1. Data from *Pst*, *Pc* and no-choice *Sl* assays, hyperspectral imaging, glucosinolate profiling and RT-qPCR experiments were analysed by linear models. If data showed normal distributions and homoscedasticity, the analysis was performed by two-sample t-tests (binary comparisons) or one-, two- or three-way ANOVAs followed by Tukey post-hoc tests (multiple groups). Welch two-sample t-tests were used when binary comparison data showed heteroscedasticity. If data showed heteroscedasticity and/or residuals did not follow a normal distribution, data were transformed (logged, squared, square-rooted or transformed with the Box-cox or Yeo-Johnson transformations). When transformations failed to yield normal distributions, data were analysed by non-parametric Mann-Whitney tests (binary comparisons) or Kruskal-Wallis tests followed by Pairwise Wilcoxon Rank Sum Tests (multiple groups) with *p*-values adjusted using the FDR approach. In all cases, a difference was deemed statistically significant at $p < 0.05$. To test for statistically significant changes in larval attractiveness in the dual-choice *Sl* assays, total numbers of larvae choosing plants from water- or JA-treated seedings were analysed by a Goodness-of-fit test against the null hypothesis that larval numbers were equal across treatments ($p < 0.05$).

REFERENCES

1. López Sánchez, A., Stassen, J. H. M., Furci, L., Smith, L. M. & Ton, J. The role of DNA (de)methylation in immune responsiveness of Arabidopsis. *Plant J.* **88**, 361–374 (2016).

2. Smith, M. R. *et al.* Cyclophilin 40 is required for microRNA activity in *Arabidopsis*.

Proc. Natl. Acad. Sci. U. S. A. **106**, 5424–5429 (2009).

3. Fernández-Calvo, P. *et al.* The *Arabidopsis* bHLH transcription factors MYC3 and MYC4 are targets of JAZ repressors and act additively with MYC2 in the activation of jasmonate responses. *Plant Cell* **23**, 701–715 (2011).

4. Gupta, G. P., Rani, S., Birah, A. & Raghuraman, M. Improved artificial diet for mass rearing of the tobacco caterpillar, *Spodoptera litura* (Lepidoptera: Noctuidae). *Int. J. Trop. Insect Sci.* **25**, 55–58 (2005).

5. Roeder, K. A., Kuriachan, I., Vinson, S. B. & Behmer, S. T. Evaluation of a microbial inhibitor in artificial diets of a generalist caterpillar, *Heliothis virescens*. *J. Insect Sci.* **10**, 197 (2010).

6. Bricchi, I. *et al.* Separation of early and late responses to herbivory in Arabidopsis by changing plasmodesmal function. *Plant J.* **73**, 14–25 (2013).

7. Brunel, D. An alternative, rapid method of plant DNA extraction for PCR analyses. *Nucleic Acids Res.* **20**, 4676 (1992).

8. Siligato, R. *et al.* Multisite gateway-compatible cell type-specific gene-inducible system for plants. *Plant Physiol.* **170**, 627–641 (2016).

9. Zuo, J., Niu, Q. W. & Chua, N. H. An estrogen receptor-based transactivator XVE mediates highly inducible gene expression in transgenic plants. *Plant J.* **24**, 265–273 (2000).

10. Harrison, S. J. *et al.* A rapid and robust method of identifying transformed *Arabidopsis thaliana* seedlings following floral dip transformation. *Plant Methods* **2**, 19 (2006).

11. Hooshmand, K. & Fomsgaard, I. S. Analytical Methods for Quantification and Identification of Intact Glucosinolates in Arabidopsis Roots Using LC-QqQ(LIT)-MS/MS. *Metabolites* **11**, 47 (2021).

12. Furci, L. *et al.* Identification and characterisation of hypomethylated DNA loci controlling quantitative resistance in *Arabidopsis*. *Elife* **8**, e40655 (2019).

13. Ewels, P., Magnusson, M., Lundin, S. & Käller, M. MultiQC: summarize analysis results for multiple tools and samples in a single report. *Bioinformatics* **32**, 3047–3048 (2016).

14. Bolger, A. M., Lohse, M. & Usadel, B. Trimmomatic: a flexible trimmer for Illumina sequence data. *Bioinformatics* **30**, 2114–2120 (2014).

15. Dobin, A. *et al.* STAR: ultrafast universal RNA-seq aligner. *Bioinformatics* **29**, 15–21 (2013).

16. Anders, S., Pyl, P. T. & Huber, W. HTSeq - a Python framework to work with high-throughput sequencing data. *Bioinformatics* **31**, 166–169 (2015).

17. Anders, S. & Huber, W. Differential expression analysis for sequence count data. *Genome Biol.* **11**, R106 (2010).

18. Love, M. I., Huber, W. & Anders, S. Moderated estimation of fold change and dispersion for RNA-seq data with DESeq2. *Genome Biol.* **15**, 550 (2014).

19. Krueger, F. & Andrews, S. R. Bismark: a flexible aligner and methylation caller for Bisulfite-Seq applications. *Bioinformatics* **27**, 1571–1572 (2011).

20. Langmead, B. & Salzberg, S. L. Fast gapped-read alignment with Bowtie 2. *Nat. Methods* **9**, 357–359 (2012).

21. Li, H. *et al.* The Sequence Alignment/Map format and SAMtools. *Bioinformatics* **25**, 2078–2079 (2009).

22. Stuart, T., Buckberry, S. & Lister, R. Approaches for the analysis and interpretation of whole genome bisulfite sequencing data. in *Epigenome Editing: Methods and Protocols, Methods in Molecular Biology* (eds. Jeltsch, A. & Rots, M. G.) 299–310

(Humana Press, 2018).

23. Schultz, M. D., Schmitz, R. J. & Ecker, J. R. 'Leveling' the playing field for analyses of single-base resolution DNA methylomes. *Trends Genet.* **28**, 583–585 (2012).

24. Feng, H., Conneely, K. N. & Wu, H. A Bayesian hierarchical model to detect differentially methylated loci from single nucleotide resolution sequencing data. *Nucleic Acids Res.* **42**, e69 (2014).

25. Wu, H. *et al.* Detection of differentially methylated regions from whole-genome bisulfite sequencing data without replicates. *Nucleic Acids Res.* **43**, e141 (2015).

26. Quinlan, A. R. & Hall, I. M. BEDTools: a flexible suite of utilities for comparing genomic features. *Bioinformatics* **26**, 841–842 (2010).

27. Tang, K., Lang, Z., Zhang, H. & Zhu, J. K. The DNA demethylase ROS1 targets genomic regions with distinct chromatin modification. *Nat. Plants* **2**, 16169 (2016).

28. Ni, P. *et al.* Genome-wide detection of cytosine methylations in plant from Nanopore data using deep learning. *Nat. Commun.* **12**, 5976 (2021).

29. Thorvaldsdóttir, H., Robinson, J. T. & Mesirov, J. P. Integrative Genomics Viewer (IGV): high-performance genomics data visualization and exploration. *Brief. Bioinform.* **14**, 178–192 (2013).

30. Czechowski, T., Stitt, M., Altmann, T., Udvardi, M. K. & Scheible, W. R. Genome-wide identification and testing of superior reference genes for transcript normalization in Arabidopsis. *Plant Physiol.* **139**, 5–17 (2005).

31. Camacho, C. *et al.* BLAST+: architecture and applications. *BMC Bioinformatics* **10**, 421 (2009).

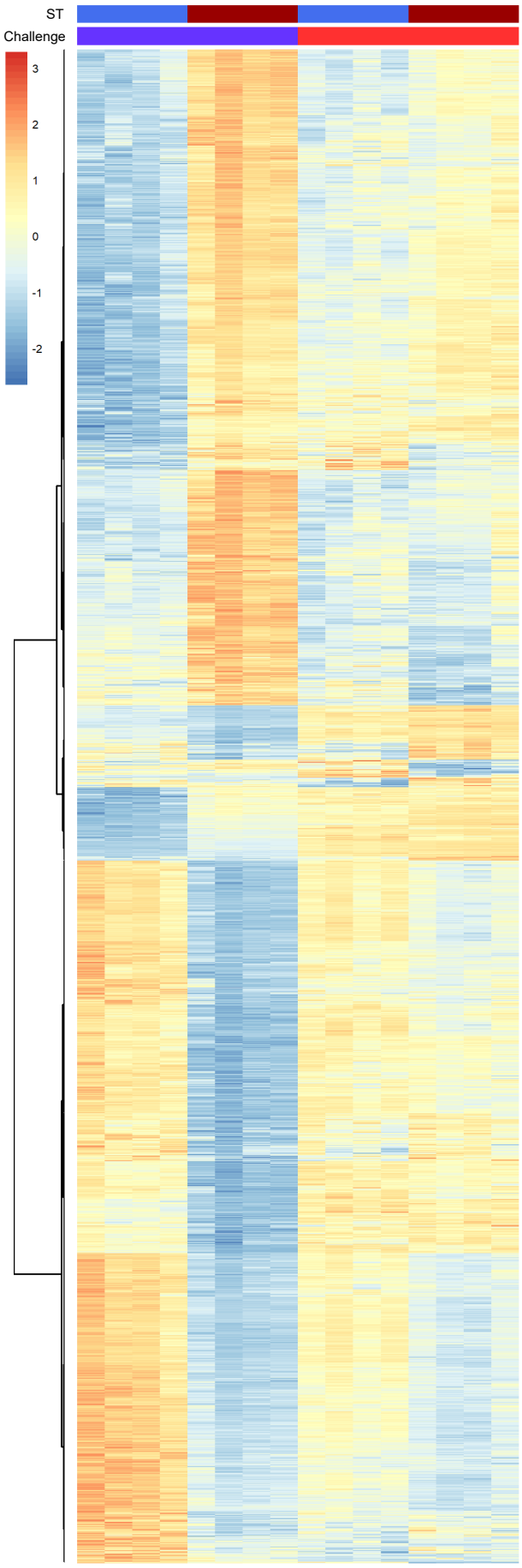

Supplementary Fig. 1 | Selection of genes showing altered JA responsiveness to JA challenge in 5-week-old plants as a consequence of JA seedling treatment. Expression profiles of 2,409 genes with a statistically significant interaction between seedling treatment (ST) and challenge treatment (*p.adj* < 0.01). Replicate samples (*n*=4) for mRNA-seq analysis were collected from 5-week-old plants at 4 hrs after challenge with water (W) or 0.1 mM JA. Plants had been pre-treated with water or 1 mM JA at the seedling stage (2-week-old). Blue and red columns above the heatmap indicate water and JA treatments, respectively. Heatmap-projected values represent per gene z-scores of transformed read counts from all biological replicates.

Supplementary Table 1 | Ingredients of the *Spodoptera littoralis* diet.

Ingredient	Amount	Supplier	Product code
Haricot Beans	125 g	Real foods	NA
Agar	20 g	NEOGEN	MC006
Ascorbic Acid	4 g	Sigma Aldrich	A1417
Multivitamin A-Z Daily Tablets	2 Tablets	Lindens Health and Nutrition	5060332533763
Ethyl 4-hydroxybenzoate	2.25 g	Sigma Aldrich	111988
Formaldehyde Solution (approx. 35-40% Formaldehyde)	325 µl	Sigma Aldrich	F8775
Propionic Acid	836 µl	BDH	296884k
Phosphoric Acid Solution	84 µl	Sigma Aldrich	W290017
Sorbic Acid	0.016 g	Sigma Aldrich	S1626
Benzoic Acid	0.008 g	Sigma Aldrich	242381
Chloramphenicol	0.002 g	BioVision	2486
Distilled Water	600 ml	NA	NA

Supplementary Table 2 | RT-qPCR primers.

Target Gene	Forward primer (5'-3')	Reverse primer (5'-3')	Reference
VSP2 *AT5G24770*	GGACTTGCCCTAAAGAACGACACC	GTCGGTCTTCTCTGTTCCGTATCC	This Study
PDF1.2 *AT5G44420*	CTTGTTCTCTTTGCTGCTTTCGAC	TTGGCTCCTTCAAGGTTAATGCAC	This Study
PR1 *AT2G14610*	ACACGTGCAATGGAGTTTGTGG	TTGGCACATCCGAGTCTCACTG	This Study
MYC2 *AT1G32640*	AACCACGTCGAAGCAGAGAGAC	TTGGTACAACCGCTCGTAACGC	This Study
ROS1 *AT2G36490*	AAAACTACCCCTCATCGCTG	GTTAGTACGTGCATATTCCAAGC	[1]
GAPC2 *AT1G13440*	GCCATCCCTCAATGGAAAATT	GAGACATCAACGGTTGGAACA	This Study
UBC21 *AT5G25760*	CTGCGACTCAGGGAATCTTCTAA	TTGTGCCATTGAATTGAACCC	[2]
MON1 *AT2G28390*	AACTCTATGCAGCATTTGATCCACT	TGATTGCATATCTTTATCGCCATC	[2]

References

1. Duan, C. G. *et al.* MET18 Connects the Cytosolic Iron-Sulfur Cluster Assembly Pathway to Active DNA Demethylation in Arabidopsis. *PLoS Genet.* **11**, e1005559 (2015).
2. Czechowski, T., Stitt, M., Altmann, T., Udvardi, M. K. & Scheible, W.-R. Genome-wide identification and testing of superior reference genes for transcript normalization in Arabidopsis. *Plant Physiol.* **139**, 5–17 (2005).